

Integrated Master in Bioengineer

Effects of peptides on the structure of lipid bilayers: Implication for its therapeutic effect in Alzheimer's disease

Catarina Helena da Silveira Miranda Guedes Pimentel

Master thesis realized under the Branch of Biological Engineer

Advisor: **Prof. Dr^a. Maria do Carmo Pereira**

Co-advisor: **Dr^a. Joana Angélica Loureiro**

Departamento de Engenharia Química

July 2017



For my Mother, I can't see her... But I know that she is always there.

*"So far away from where you are
These miles have torn us worlds apart
And I miss you, yeah I miss you
So far away from where you are
I'm standing underneath the stars
And I wish you were here
I miss the years that were erased
I miss the way the sunshine would light up your face
I miss all the little things
I never thought that they'd mean everything to me
Yeah I miss you
And I wish you were here
I feel the beating of your heart
I see the shadows of your face
Just know that wherever you are
Yeah, I miss you
And I wish you were here"*

Jason Wade, Lifehouse

Acknowledgements

First of all, I would like to thank my supervisor, Prof. Dr^a. Maria do Carmo Pereira, for giving me the opportunity to work in their research group, for the guidance provided, and encouragement at all times. I would also like to express my thanks to Dr^a. Joana Loureiro for the constant support, scientific guidance and all the availability throughout the development of this work.

I wish to acknowledge to my investigation group colleagues for their support and help, sharing of ideas and all moments experienced in work and out work. Additionally, I want to send an especial thanks to Stéphanie Andrade for the constant support, for all your comprehension and availability at every moment.

I'm also especially thankful to Ana Rodrigues and Isabel Oliveira, that always supported me and followed this journey, but the most important for me, they always believed in me. From my heart, my sincere thanks.

Also, I would like to say thanks to my friends from UTAD: Margarida Moura and Luís Costa for all support, all the laughter and, above all, for their friendship. I also wish to express my sincere thanks to my heartfelt brother, house mate during all course, and companion of all hours throughout all these difficult years, Ivo Barros, for the love shown, unconditional support, unfailing friendship that pulls me a smile when a tear overlaps. Thank you from the heart.

Additionally, I would like to express my sincere thanks from the bottom of my heart to my "aunts" from Lisbon: Sandra Martins, Patricia Isabel, Catarina Oliveira, Susana Miguel and Sara Pereira for the unconditional support in the most difficult phase of my life, who accompany me since ever and forever with their encouraging smile, their lessons of life, their tight embrace and unconditional love.

Likewise, I would like to express my gratitude to the Podence family, who sheltered me here in Porto this year, with all the readiness, care and dedication. They are a family to me.

Finally, but not least, I wish to extend my profound thanks to my family, for always believing in me and what I do. My most special thanks go to my father, Paulo Pimentel, for all his tireless efforts, affection, dedication and love so that this dream could be fulfilled. Also to my little brother, Rodrigo Pimentel, the reason of my life, which without knowing, never let me fall with an unconditional smile and a tight hug, thank you from the bottom of my heart. Without you, none of this would be possible. I hope this step that I finish now, allow some way, reciprocate and compensate for everything that you have done for me.

To my mother, Helena Pimentel, my force and my person: the objective is fulfilled. I hope I have left you as proud as possible, always with our smile.

I also place on record, my sense of gratitude to one and all, who directly or indirectly, gave a little about yourself to this project.

This work was in part funded by projects (i) POCI-01-0145-FEDER-006939 (Laboratório de Engenharia de Processos, Ambiente, Biotecnologia e Energia, UID/EQU/00511/2013) - funded by FEDER through COMPETE2020 - Programa Operacional Competitividade e Internacionalização (POCI) – and by national funds through FCT - Fundação para a Ciência e a Tecnologia and (ii) NORTE-01-0145-FEDER-000005 – LEPABE-2-ECO-INNOVATION, funded by FEDER - Fundo Europeu de Desenvolvimento Regional, through COMPETE2020 – Programa Operacional Competitividade e Internacionalização (POCI) and Programa Operacional Regional do Norte (NORTE2020).

Prof. Dr^a. Maria do Carmo Pereira, supervisor of this work, is a member of LEPABE – Laboratório de Engenharia de Processos, Ambiente, Biotecnologia e Energia, funded by Projects (i) POCI-01-0145-FEDER-006939 (Laboratório de Engenharia de Processos, Ambiente, Biotecnologia e Energia, UID/EQU/00511/2013) - funded by FEDER through COMPETE2020 - Programa Operacional Competitividade e Internacionalização (POCI) – and by national funds through FCT - Fundação para a Ciência e a Tecnologia and (ii) NORTE-01-0145-FEDER-000005 – LEPABE-2-ECO-INNOVATION, funded by FEDER - Fundo Europeu de Desenvolvimento Regional, through COMPETE2020 – Programa Operacional Competitividade e Internacionalização (POCI) and Programa Operacional Regional do Norte (NORTE2020).

Abstract

Alzheimer's disease (AD), which is characterized by progressive memory loss and cognitive function, is considered to be the most common neurodegenerative disease in the world. This type of dementia mainly reach the elderly population, which has been increasing significantly. Over 46 million people live with dementia worldwide. This number is estimated to increase to 131.5 million by 2050.

It is very important to identify signs of risk in order to early detect the disease. There is currently no cure for this disease, and the existing treatments focus only on relieving symptoms rather than reversing the disease. AD is characterized by the presence of neurofibrillary tangles (Tau protein) and amyloid plaques, whose the main component is the amyloid- β (A β) peptide that may result from mutations in the amyloid precursor protein (APP) gene.

The blood-brain barrier (BBB) defines the interface between the bloodstream and the brain, preventing the entry of most molecules and cells, thereby maintain the central nervous system homeostasis. Due to the presence of this barrier, drug delivery therapy through the brain becomes a major challenge.

Liposomes were used as membrane model to study the interactions between the cell membrane and the therapeutic peptides, A β PepInib and LP γ FFD-PEG (beta-sheet breaker peptides previously designed by the research team). In addition, to reach a greater approximation with the complexity of the cell membrane, cholesterol was added to this system.

The A β PepInib sample was analyzed by mass spectrometry and transmission electron microscopy, providing morphological characteristics of the aggregates. Fluorescence quenching and absorption spectrophotometry techniques were chosen to evaluate the interaction between the membrane and the related compounds. The membrane fluidity was studied through the measurement of phase transition temperature.

The interaction studies clear evidence the interaction between the peptides and the model membrane. It is further seen that they interact favorably by electrostatic interactions preferring a surface location, since they had no affinity with the deeply located probe. It is also important mentioning the clear difference between the values of the system with and without cholesterol, which are lower in the presence of cholesterol that demonstrates its condensation and organization effect of the cell membrane.

✓ **Keywords:** Alzheimer's disease; Peptides; Biomembrane models; A β PepInib; LP γ FFD-PEG.

Resumo

A doença de Alzheimer, caracterizada por progressivas perdas de memória e função cognitiva, é considerada a doença neurodegenerativa mais comum em todo o mundo. Com o aumento da esperança média de vida, este tipo de demência tem aumentado ao longo dos anos. Em todo o mundo, mais de 46 milhões de pessoas padecem desta doença, e espera-se que este número aumente para 131.5 milhões em 2050.

É muito importante a identificação precoce de sinais de risco para que se possa detetar o estágio inicial da doença, para que as intervenções terapêuticas se possam tornar mais eficientes. Atualmente não há cura para esta doença, e os tratamentos existentes focam-se apenas no alívio dos sintomas e não na sua reversão. A doença de Alzheimer é caracterizada pela presença de emaranhados neurofibrilares (proteína Tau) e placas de amilóide, cujo principal componente é o péptido amilóide β ($A\beta$) que pode ser resultado de mutações no gene da proteína precursora de amilóide.

A barreira hematoencefálica define a interface entre a corrente sanguínea e o cérebro impedindo a entrada da maioria das moléculas e células mantendo assim a homeostasia do sistema nervoso central. Devido à presença desta barreira a entrega de fármacos no cérebro torna-se assim um grande desafio.

Neste trabalho lipossomas foram utilizados como modelo para estudar as interações entre a membrana celular e os péptidos terapêuticos, *A β PepInib* e LP γ FFD-PEG (péptidos específicos para a quebra de folha β previamente desenhados pelo grupo de investigação). Adicionalmente e para atingir uma maior aproximação com a complexidade da membrana celular adicionou-se a este sistema colesterol.

A amostra de *A β PepInib* foi analisada por espectrometria de massa e microscopia eletrónica de transmissão, providenciando características morfológicas dos agregados. As técnicas de *fluorescence quenching* e espectrofotometria de absorção foram escolhidas para avaliar a interação entre a membrana e os referidos compostos. A fluidez da membrana foi estudada através da medição da temperatura de transição de fase.

Os estudos realizados evidenciam a interação entre péptidos e o modelo membranal. Verificou-se ainda, que interagem preferencialmente por interações eletrostáticas adotando uma localização superficial. De referir também a nítida diferença entre os valores do sistema membranal com e sem colesterol, revelando estes serem mais baixos no caso da presença de colesterol o que comprova o seu efeito de condensação e organização da membrana celular.

✓ **Palavras-chave:** Doença de Alzheimer; Péptidos; Modelos biomembranares; *A β PepInib*; LP γ FFD-PEG.

Declaração/Declaration

Declara, sob compromisso de honra, que este trabalho é original e que todas as contribuições não originais foram devidamente referenciadas com identificação da fonte.

Declare, under oath, that this work is original and that all non-original contributions were properly referenced with the source identification.

Porto, 20 junho de 2017 | Oporto, 20th june 2017

(Catarina Helena da Silveira Miranda Guedes Pimentel)

Contents

Acknowledgements.....	v
Abstract	vii
Resumo.....	ix
Declaração/Declaration.....	xi
List of figures	xv
List of tables	xvii
Abbreviations and Symbols.....	xix
INTRODUCTION	1
Motivation.....	1
Main Objective	2
Thesis Organization	2
STATE OF THE ART	5
Alzheimer disease	5
Amyloid Cascade Hypothesis	6
Brain Blood Barrier	8
Cell Membrane.....	10
Models of Membranes	11
Drugs on Alzheimer's disease treatment	14
Fluorinated Compounds.....	16
Peptides for Alzheimer Disease.....	17
MATERIALS AND METHODS	21
Materials	21
Methods	22
RESULTS AND DISCUSSION.....	31
Peptide Characterization.....	31
Structural Analysis of Amyloid beta Peptide.....	32
Liposomes Characterization	33
Determination of Partition Coefficient by Derivative Spectrophotometry	33
Phase Transition Temperature Studies	38
Drug Location Studies by Fluorescence Quenching	41
CONCLUDING REMARKS AND FUTURE PERSPECTIVES.....	44
REFERENCES	46

List of figures

Figure 1 - Processing of APP into A β peptides with further development of ACH. (Adapted by (Stahl and Muntner 2013)).....	8
Figure 2- Differences between blood capillaries and brain capillaries (BBB): endothelial cells held together by tight junctions (TJs) that form a highly selective barrier between the blood supply and the cerebral spinal fluid. Adapted by (Esparza).....	10
Figure 3 - Model of lipid monolayers at the air-water interface. (Adapted by (Chen and Bothun 2013)).....	12
Figure 4 - SLBs as a model to mimic the lipid bilayer of the biological membrane. (Adapted by (Chen and Bothun 2013)).....	13
Figure 5 - Liposome as a lipid vesicle with the core hydrophilic cover by the lipid bilayers (lipophilic). (Adapted by (Chen and Bothun 2013)).....	14
Figure 6 - Schematic representation of the main liposomal drugs and targeting agents that improve liposome affinity and selectivity for brain delivery. Adapted by (Vieira and Gamarra 2016)	16
Figure 7 - Chemical Structure of LP β FFD-PEG peptide. (Marvin Software).....	22
Figure 8 - Principle of transmission electron microscopy (Adapted by Enciclopedia Britannica, Inc.).....	23
Figure 9 - TOF MS of the A β PepInib peptide.....	31
Figure 10- Transmission Electron Microscopy images of the effect of A β PepInib peptide on the A β ₍₁₋₄₂₎ aggregation. The samples were incubated for 24 hours, and the figure present 3 time points: 0 h, 6 h and 24 h. The scale bar correspond to 100 nm.....	32
Figure 11 - Absorption spectra (A) and second-derivative spectra (B) of A β PepInib (600 μ M) incubated in LUVs of DMPC at 37 $^{\circ}$ C (gray lines) and LUVs of DMPC without drug (black lines) at increasing lipid concentrations (n=3). The curve C represents the best fit by Eq. (4)	35
Figure 12 - Absorption spectra (D) and third-derivative spectra (E) of LP β FFD-PEG (15.26 μ M) incubated in LUVs of DMPC at 37 $^{\circ}$ C (gray lines) and LUVs of DMPC without drug (black lines) at increasing lipid concentrations. The curve F represents the best fit by Eq. (4) (n=2)	36
Figure 13 - Normalized mean count rate of DMPC and DMPC:Peptide (left) and DMPC:Chol and DMPC:Chol:Peptide (right) at pH 7.4 as function of temperature.....	39
Figure 14 - Stern-Volmer plots obtained by steady-state fluorescence measurements of DPH in LUVs of DMPC (for both peptides), and DMPC:Chol (only for A β PepInib) under physiological conditions (pH 7.4; 37 $^{\circ}$ C).....	42

List of tables

Table 1 - Protein and lipid content in wild type (WT) mouse brains. Data were derived by the analysis of three different brains and are expressed as means values \pm S.D. f.t., (fresh tissue). Transcribed by Scandroglio <i>et al.</i> (Scandroglio et al. 2008).....	11
Table 2 - AD Therapeutic Peptides: The Peptide Category, Name, Sequence, Description and Related References.	18
Table 3 - Chemical structure of the compounds used to prepare liposomes (by Sigma Aldrich)24	
Table 4 - Mean diameter, PDI and Zeta Potential of the liposomes with and without cholesterol (n=3;*n=2)	33
Table 5 – Partition coefficients values obtained for A β PepInib expressed as K _p and logD (n=3; *n=2)	36
Table 6 - Partition coefficients values obtained for LP _f FFD-PEG expressed as K _p and logD (n=2)	37
Table 7 - Values of main phase transition temperature (T _m) obtained from DMPC, DMPC:Chol at pH 7.4 in the absence and presence of peptides, obtained by fitting eq 5. (n=3; *n=2).....	39
Table 8 - Values of Stern-Volmer constant at T = 37 °C obtained for peptides in DMPC labeled with DPH probe. (n=2).....	42

Abbreviations and Symbols

ACH:	Amyloid cascade hypothesis
AD:	Alzheimer's Disease
AFM:	Atomic force microscopy
AMPs:	Antimicrobial peptides
AP:	Amyloid plaques
APP:	Amyloid precursor protein
A β :	Amyloid- β peptide
A β PepInib:	Amyloid- β peptide inhibitor
BBB:	Blood-brain barrier
B-CSFB:	Blood-cerebrospinal fluid barrier
CF:	Chloroform
Chol:	Cholesterol
CNS:	Central nervous system
CPPs:	Cell penetrating peptides
CSF:	Cerebrospinal fluid biomarkers
D or Asp:	Aspartic Acid
DLS:	Dynamic light scattering
DMSO:	Dimethyl sulfoxide
DN:	Dystrophic neurites
DPH:	1,6-diphenyl-1,3,5- hexatriene
DS:	Down's syndrome
DSC:	Differential scanning calorimetry
EPR:	Enhanced permeability and retention
F or Phe:	Phenylalanine
FAD:	Familial AD
FTIR:	Fourier transform infrared spectroscopy
GFAP:	Glial fibrillary acidic protein
HFIP:	1,1,1,3,3,3-hexafluoro-2-propanol
IWG:	International Working Group
K _p :	Partition coefficients
K _{sv} :	Stern-Volmer constant
L or Leu:	Leucine
L _d :	Liquid disordered phase
L _o :	Liquid-ordered phase
LPFFD:	Leu-Pro-Phe-Phe-Asp
LP _r FFD:	Leu-FluoroPro- Phe-Phe-Asp

MCI: Mild cognitive impairment

MS: Mass Spectrometry

NFTs: Neurofibrillary tangles of hyperphosphorylated Tau

NIA-AA: National Institute of Aging and Alzheimer's

NMDA: N-methyl-D-aspartate

NP: Nanoparticle

P or Pro: Proline

PA: Phosphatidic acid

PBS buffer: Phosphate buffered saline

PC: Phosphatidylcholine

PdI: Polydispersity index

PE: Phosphatidylethanolamine

PEG: Polyethylene glycol

pI: Isoelectric point

pKa: acid dissociation constant

PLs: Phospholipids

PMs: Plasma Membranes

PS: Phosphatidylserine

PSEN: Presenilin genes

SIMS: Secondary Ion mass spectrometry

SLBs: Supported Lipid bilayers

SP: Senile plaques

TEM: Transmission Electron Microscopy

TJs: Tight junctions

TOF: Time-of-Flight

ζ-Potential: Zeta Potential

Chapter 1

INTRODUCTION

Motivation

Alzheimer's Disease (AD) is the most common type of dementia in the world affecting more than 45 million people in 2015. Expectations leads to a significance increase of this number (M. Prince 2015). AD is characterized by neuronal death that causes progressive loss of memory and cognition, changes behavior or personality, and ability to think clearly. Ultimately is fatal.

The pathological features of this disease include the formation of neuritic plaques composed of amyloid- β peptide ($A\beta$) fibrils and neurofibrillary tangles of hyperphosphorylated Tau protein. The extracellular deposition of the $A\beta$ peptide precedes cerebral atrophy and the great decline at the cognitive level (Nordberg 2004; Villemagne et al. 2013).

Despite all the advances made in researching new therapies for AD, current treatments are based on reducing patient symptoms rather than healing. Most of the drugs tested for AD fail due to the existence of the blood-brain barrier (BBB) that restrain the drugs to reach the brain (Lockman 2002).

The development of molecules based on products of natural source and small molecular sizes had a significant impact in the improvement of new drugs. In this regard, fluorine which is characterized by being an atom of small dimensions and with very high electronegativity was of paramount relevance. The substitution of this atom has been increasingly verified in chemical medicine for demonstrating improvements in metabolic stability, bioavailability and protein-ligand interactions (Purser et al. 2008). An intense flow of fluorine compounds in the pharmaceutical industry has brought immense advances, including steroidal and nonsteroidal anti-inflammatory drugs, central nervous system drugs, anticancer agents and antiviral agents. A very important fact is that it has been proved that organofluorinated compounds with highly negative zeta potential and hydrophobic fluorinated core have the fundamental characteristics to prevent $A\beta$ fibrillogenesis, thus revealing a promising interest for the treatment of AD (Rocha et al. 2008).

Due to all complexity of biological membranes, these become challenging to study in real situations. The artificial membrane systems that mimic the natural lipid bilayer membranes (Eeman and Deleu 2010) have been target of intense research to simulate behavior *in vivo*.

Several models have been developed for the study of membrane properties, structure and processes, as well as the study of their interaction with natural or synthetic forms of compounds such as surfactants, peptides and drugs. The most studied and used systems for this purpose are lipid monolayers, supported lipid bilayers and liposomes.

Liposomes more easily demonstrate the complexity of the biological membrane structure once they are arranged in a very similar way to the cell membrane. Liposomes represent a membrane model widely used in the characterization and investigation of lipid interactions in nanosystems. Due to their exclusive characteristics, namely, their capacity to incorporate hydrophilic and hydrophobic drugs, good biocompatibility, and low toxicity, have been the most used as the cell membrane model (Spuch and Navarro 2011; Caracciolo and Amenitsch 2012).

Main Objective

The aim of this work was to study how the therapeutic peptides for the AD affect the membrane order and structure. Particular emphasis was given on the interactions of these compounds with the lipidic models used to simulate the cell membrane.

The morphological structure of A β in presence of the therapeutic peptides was investigated by Transmission electron microscopy (TEM) analysis, and sequence of A β PeptInib was accessed by Time-of-flight mass spectrometry (TOF MS).

The behavior of peptides in biomembrane models was assessed by determination of the partition coefficients by spectrophotometry using liposomes/water systems. The location of the therapeutic peptides in the model membranes was studied by fluorescence quenching of the probe with a well-known location. The influence of peptides in the organization and fluidity of the membrane was assessed by dynamic light scattering (DLS).

It is also an objective to understand and evaluate the drug-cell membrane interactions. These interactions may aid the general understanding of the pharmacokinetics of the studied and potential therapeutic peptides.

Thesis Organization

The present thesis is organized into five chapters. The first chapter is the *Introduction*, and it is where the motivation and main objectives of this research work are presented. The second chapter, *State of the Art*, follows through an overview of the AD, the amyloid cascade hypothesis, the BBB, a review of models of membranes and drug delivery systems, and an

overview about fluorinated compounds and peptides for AD. The *Materials and Methods* chapter focuses on the material and techniques used for the accomplishment of the work. The relevant results and their discussion are presented in the *Results and Discussion* section. The last chapter, *Conclusions and Future Perspectives* will present the conclusions drawn on the basis of the results obtained. Finally, in *Appendix* all the further results are included.

Chapter 2

STATE OF THE ART

Alzheimer disease

Dementia is a generic term that describes conditions or diseases that develop when nerve cells in the brain (called neurons) die or no longer function normally. AD is the most common type of dementia. AD causes progressive loss of memory and cognition, changes behavior or personality, and ability to think clearly. This fatal disease in an advanced stage can inclusively impair an individual's ability to carry out basic bodily functions as walking and swallowing.

This disease mainly reaches the population over 65 years old. 9.9 million new cases of dementia arise in the world, one for every 3 seconds. Between 2000 and 2010 there was a decrease in the proportion of deaths resulting from heart disease, stroke and prostate cancer by about 16%, 23% and 8%, respectively, while the opposite occurred in Alzheimer's disease which increased in about 68%. In the United States, in 2010, was the sixth leading cause of death (Alzheimer's 2014). By 2015, the number of people with dementia was around 46.8 million worldwide, but expectations for 2050 are around 131.5 million. In terms of regional distribution, the new cases of dementia were about 4.9 million (49% of the total) in Asia, 2.5 million (25%) in Europe, 1.7 million (18%) in America, and 0.8 million (8%) in Africa.

As mentioned earlier, the disease's standard symptom is the difficulty of remembering new information due to the death or malfunction of the neurons in brain regions that involve the formation of these memories. Further difficulties arise because the same occurs in neurons in other brain regions (Alzheimer's 2014). In general, functional, structural, and biochemical abnormalities appear one or two decades before the onset of dementia symptoms develops. Even before individuals report any symptoms, longitudinal neuropsychological studies indicate that cognitive impairment has already begun about a decade ago. This suggests that AD, like many other chronic diseases characteristic of aging, consists of a first asymptomatic phase followed by a symptomatic phase (Lesné et al. 2013).

The causes of AD are for now unknown, however genetic studies suggest that it is due to the formation of two well-known aggregate abnormalities. The pathological features of this disease include the formation of neuritic plaques composed of A β peptide fibrils,

neurofibrillary tangles of hyperphosphorylated Tau (NFTs), and neurotransmitter deficits (Butterfield and Lauderback 2002; Alzheimer's 2014). Neuropathological, genetic and molecular data suggest that the binding protein of Tau microtubules mediates the disease process (Jack et al. 2013). The neurodegeneration pattern correlates with Tau neuropathy and measures amyloid- β -induced neurotoxicity.

Alois Alzheimer, author and recognizer of the neurodegenerative disease that later acquired his name, described the presence of amyloid plaques (AP) and neurofibrillary tangles in the brain (Nordberg 2004). Nowadays AD is fundamentally characterized by the accumulation of the A β peptide and intracellular neurofibrillary tangles, in addition to neuronal and synaptic losses and neurotransmitter deficits (Hardy and Selkoe 2002).

Amyloid Cascade Hypothesis

John Hardy and his colleagues, in 1992, postulated the hypothesis of the amyloid cascade (ACH) that in the last 25 years has been shown to be the most influential model with a fundamental role in the pathology of Alzheimer's disease. In this hypothesis, A β peptide represent the most important constituent of senile plaques (SP) (Figure 1) (A. Armstrong 2014; Hardy and Selkoe 2002).

A β peptide is present in the form of small insoluble peptides and when deposited it forms deposits classified as neuritic plaques, amyloid angiopathy of the capillaries or diffuse amyloid deposits. These deposits are early and mandatory events of AD.

A β peptide represents a normal product of APP metabolism and could be measured in culture medium, cerebrospinal fluid and plasma. This way the scientists quickly understood the biochemical abnormalities caused by APP mutations (Hardy and Selkoe 2002).

The APP is a transmembrane glycoprotein of the N-terminal domain, which is expressed with broad variety in mammalian and non-mammalian cells. The A β peptide derives from this precursor, and constitutes, as already mentioned, the main protein component associated with AD (Dawkins and Small 2014; Zhao et al. 2015). Evidence of genetic mutations due to abnormality of APP processing has led to the association of ACH with overproduction of highly aggregable forms of A β_{1-42} , A β_{1-40} , amyloid fibrils and amyloid plaques (Nordberg 2004). These mutations lead to hereditary cerebral hemorrhage with amyloidosis. Generally, mutations occur grouped or close to the sites within the APP gene that are normally cleaved by proteases called α -, β -, and γ - secretases (Figure 1). The proteolytic processing of APP together with the occurrence of mutations promotes the generation of A β peptide that are toxic and can induce cell death. The toxicity can be mediated by the necrotic rather than the apoptotic

pathway. After the occurrence of changes in the proteolytic process follow events such as microglial activation, astrogliosis, dystrophic neurites (DN) and oxidative stress reactions. Three major groups of APP mutations can thus be identified: (a) the β APP cleaving enzyme 1 (β ACE1) site, (b) the γ APP cleaving enzyme site, and (c) the mid domain of the A β region.

Over the last 10 years, it has been reinforced that the most common form of early-onset FAD was linked to mutations of presenilin (PSEN) genes PSEN1 and PSEN2. This PSEN gene is composed of nine trans-membrane domains placed on the endoplasmic reticulum membrane. Initially, the endoproteolytic cleavage of PSEN and assembly into the γ -secretase complex is performed following the transport thereof to the cell surface thereby influencing APP processing. As a consequence, an increased deposition of amyloid-forming species may occur due to the possibility of the mutant PSEN1 enhance 42-specific- γ -secretase cleavage of normal APP. The opposite is verified in the absence of PSEN1 and may inhibit the normal cleavage of APP. Furthermore, it appears that PSEN1 can alter the ratio of A β species.

As support for the relation between APP and degeneration of the cytoskeleton emerges studies of FAD cases caused by APP₇₁₇ (valine-isoleucine) mutation showed them to have considerable numbers of tau-immunoreactive neurofibrillary tangles (Lantos et al. 1992).

The above mentioned peptides may induce the phosphorylation of tau by: (a) straight interacting with a domain of APP, (b) inducing tau protein kinase I with subsequently recognized of Alz-50 antibody, (c) synergisms between A β and Tau or (d) directly changing the phosphorylated state of Tau.

Some constituents that may be involved in maturation of A β deposits are secondary components of senile plaques and NFT including silicon and aluminum, acute-phase proteins such as α -antichymotrypsin, α_2 -macroglobulin and their mediator interleukin-6 (IL-6) among others. There are several proteins that can still act as *chaperones* (auxiliary proteins in the folding and unfolding of other molecular structures) leading to an increase in A β aggregation, ultimately forming a growing senile plaques.

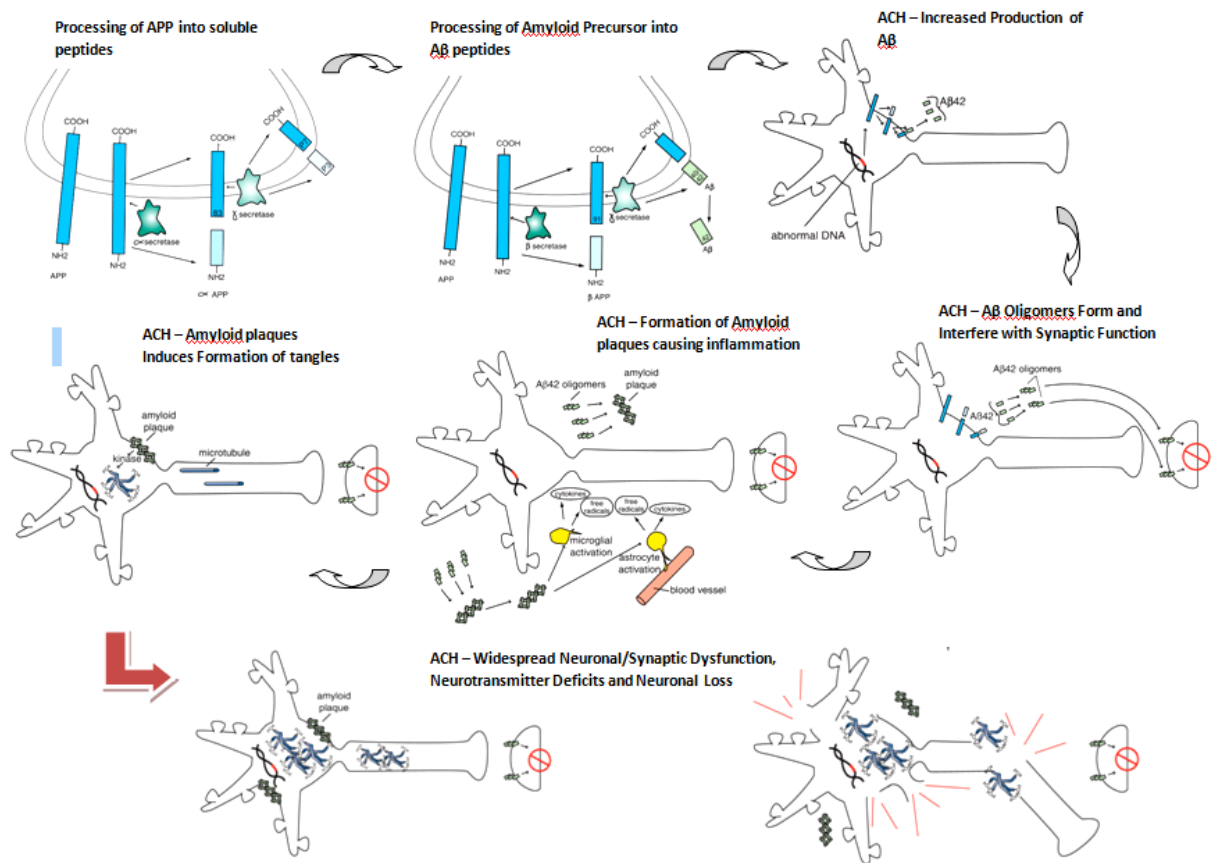


Figure 1 - Processing of APP into Aβ peptides with further development of ACH. (Adapted by (Stahl and Muntner 2013))

The molecular composition of NFT also varies according to the region where they are found and can be intracellular NFT (I-NFT) or extracellular NFT (E-NFT). E-NFT is immunoreactive for glial fibrillary acidic protein (GFAP) and Aβ; as well, it contains significant amounts of amyloid-P and ubiquitin, proteins that are acquired after degeneration of NFT-containing neurons (A. Armstrong 2014; Hardy and Selkoe 2002; Nordberg 2004). Over the years ACH remains the focus for the study and research of AD (Hardy and Selkoe 2002).

Brain Blood Barrier

The blood brain barrier (BBB) is a structure that separates the components that circulate in the blood from those occurring in the brain, thus protecting the cerebral parenchyma from harmful circulating factors. Another strong barrier of the central nervous

system (CNS) is the blood-cerebrospinal fluid barrier (B-CSFB) formed by choroid plexus and the arachnoid. They are both highly specialized structures completely differentiated from the neurovascular system. These structures are responsible for maintaining the chemical composition of the medium to ensure the proper functioning of e.g., neuronal circuits, synaptic transmission, synaptic remodeling, angiogenesis, and neurogenesis in the adult brain (Spuch and Navarro 2011; Leinenga et al. 2016).

BBB also represents a dynamic and complex system in addition to endothelial covering the cerebral capillaries. The neurons are very close to the cerebral capillaries of the CNS barriers, are rarely bigger than 20 μm diameter, and they can exert a greater control on the immediate microenvironment of the cerebral cells. BBB consists of endothelial cells, the basement membrane, pericytes, astrocytes and microglia (Figure 2). As the junctions between the endothelial cells are stretched, they restrict diffusion and the barrier system becomes involved in endocytic vesicles and consequently a low rate of transcytosis. These characteristics establish an extremely efficient paracellular and transcellular barrier. The cerebral endothelium then allows to keep BBB integrity through transendothelial transport, angiogenic capability, and allows revascularization to occur whenever necessary. Paracellular transport refers to the mechanism of passage between endothelial cells and it is utilized for ions and solutes flow. Transcellular transport is the mechanism of passage that occurs through the endothelial cells. What defines the degree of permeability in a healthy BBB is the balance between paracellular-transcellular transport (figure 2) (Saraiva et al. 2016).

BBB has the capability to restrict access to pathogens and immune cells to the brain by regulating their homeostasis. If there were no barrier there would be the possibility of fluctuations in the blood levels of e.g., water, ions, hormones and nutrients that could interrupt the activity of the neurons. To ensure that the brain receives the necessary nutrients there are mechanisms, such as active transport, that allows the passage of such molecules. The main difficulty regarding drug release at BBB is the passage of large molecules (> 400 Da) across the barrier (Nag 2003; Leinenga et al. 2016).

As previously mentioned, BBB allows a selective entry of minerals and nutrients, but confine passage to foreign substances as drugs. Thus the drug delivery system through the bloodstream will not effectively attain the brain and therefore is not useful in the treatment of CNS related diseases such as AD, Parkinson's, viral and bacterial meningitis among others. Therefore, further researches are continuing to develop approaches that act on the brain in an effective way (Spuch and Navarro 2011; Leinenga et al. 2016).

However, in recent decades and despite advances in the discovery of new drugs, there have been few developments in the prognosis of patients with neurodegenerative diseases or neurological disorders.

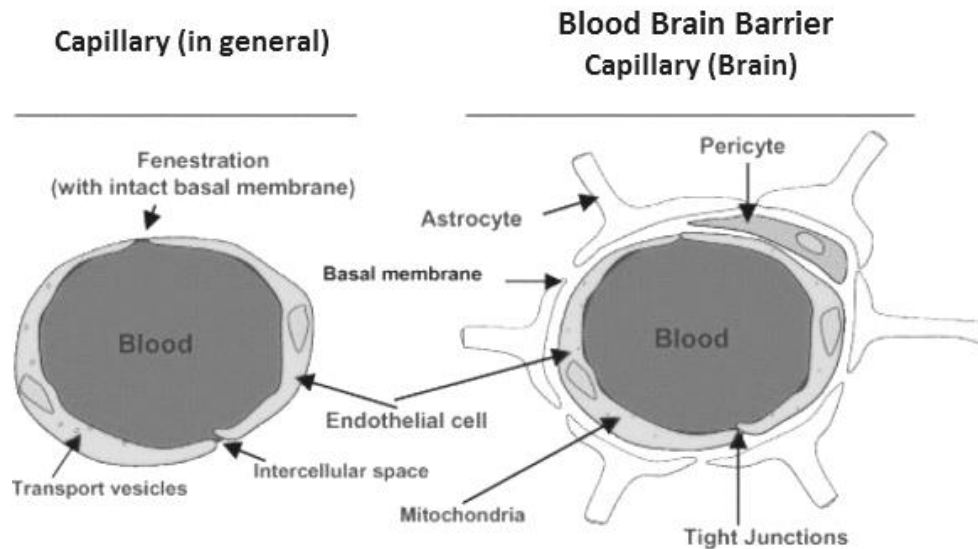


Figure 2- Differences between blood capillaries and brain capillaries (BBB): endothelial cells held together by tight junctions (TJs) that form a highly selective barrier between the blood supply and the cerebral spinal fluid. Adapted by (Esparza)

Cell Membrane

Most biologists are in agreement with the following description: “Biological membranes are continuous structures separating two aqueous phases. They are relatively impermeable to water soluble compounds, show a characteristic trilaminar appearance when fixed sections are examined by electron microscopy, and contain significant amount of lipids and proteins” (Rothfield 1971).

The cell membrane reveals a great complexity at systemic and composition level, since it is composed of a wide variety of different constituents such as lipids, carbohydrates and proteins, which vary its composition from organism to organism. The structure of membrane plays an important role in the functioning of the surrounded membrane proteins. The most relevant factor that distinguishes this membrane is the presence of a large amount of lipids, particularly phospholipids. The lipid bilayer is an underlying structure that consists in the organization from the polar headgroups facing to the aqueous environment and the hydrocarbon tails facing to the interior of the bilayer. This complex system is responsible for delimiting the cell from the external environment. Recognition and transduction into intracellular responses occur primarily at this place.

Any change that affect its structure by a bioactive molecule must be considered. A careful environmental balance has to be maintained to ensure the non-occurrence of overall effect that it may interfere on the cell membrane function and integrity.

Cell membranes are composed by three major classes of lipids: glycerolipids (mainly phospholipids), sphingolipids and sterols. In eukaryotic cell membranes, there are mainly glycerophospholipids, such as phosphatidylcholine (PC), phosphatidylethanolamine (PE), phosphatidylserine (PS) and phosphatidic acid (PA). The hydrophobic tail, whose chain length ranges from 14 to 22 carbons is saturated or cis-unsaturated (Heimburg 2007). Mammalian cells are very rich in sphingomyelin (SM) and glycosphingolipids. Cholesterol (Chol) is the sterol predominating in mammals, apparently enriched in the non-cytosolic leaflet of plasma membrane. Chol has a preferential interaction with sphingolipids, forming the so-called rafts domains (van Meer, Voelker, and Feigenson 2008). Nevertheless, between species or cell types, the lipid composition of cell membrane can show a high degree of diversity. In a generic way, table 1 shows the lipid and protein content in wild type mouse brains.

Table 1 - Protein and lipid content in wild type (WT) mouse brains. Data were derived by the analysis of three different brains and are expressed as means values \pm S.D. f.t., (fresh tissue). Transcribed by Scandroglio *et al.* (Scandroglio *et al.* 2008)

	Proteins ($\mu\text{g}/\text{mg}$ f.t.)	Cholesterol (nmol/mg f.t.)	Gangliosides (nmol/mg f.t.)	Sphingomyelin (nmol/mg f.t.)	Glycerophospholipids (nmol/mg f.t.)
WT	86.71 ± 12.21	11.40 ± 1.70	0.73 ± 0.04	1.03 ± 0.11	39.70 ± 3.02

In parallel with the lipids diversity in composition and asymmetry, different lipidic phases may still occur in the membrane depending on the structure and environment. In general, for the lamellar phases there is the possibility to observe three distinct behaviors: (I) the liquid-crystalline or liquid disordered phase characterized by the remarkable formation of glycerophospholipids with unsaturated acyl chains; (II) the solid gel phase due to SM-rich lipid mixture; (III) the liquid-ordered phase shaped by the association of sterol and bilayer-forming lipid.

Models of Membranes

Biomimetic models are an excellent alternative to study the membrane properties and its interaction with drugs under defined and controlled conditions (Knobloch *et al.* 2015; Deleu *et al.* 2014). This models arise to represent a simplified artificial membrane systems that mimic

the real cell membranes. The biomimetic models, namely lipid monolayers, lipid vesicles and supported lipid bilayers are the ones that best mimic the entire lipidic arrangement found in plasma membranes (Eeman and Deleu 2010).

- **Lipid Monolayers**

The lipids present in the membranes belong to the class of phospholipids and are typically amphiphilic molecules: they contain a hydrophobic and a hydrophilic part. A surface where one of the phases is a gas or a boundary between two immiscible phases is called the interface. The lipids are present at a polar-apolar interface orienting the hydrophilic group toward the polar phase and hydrophobic towards the apolar phase, forming a monomolecular layer.

The lipid monolayers at the air-water interface provide a simple model mimicking half-bilayer of biological membranes (Figure 3). Some of the advantages of this model in relation to complex systems, i.e. the bilayer, are that their phase state and their structure can be easily controlled by changing the molecular area through compression.

The characterization of lipid interactions with molecules of interest becomes straightforward due to the facility with which the compounds penetrate the membrane. Thus, the monolayers have been widely used for the study of peptide and protein binding and penetration, being able to observe changes in pressure or area as a function of time and concentration. It is possible to vary in a controlled way and without limitations parameters such as the nature and packaging of the molecules, composition of the sub-phase and temperature (Deleu et al. 2014; Blume and Kerth 2013).

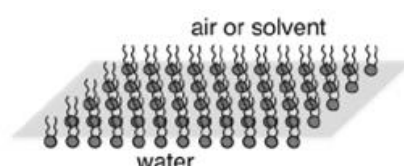


Figure 3 - Model of lipid monolayers at the air-water interface. (Adapted by (Chen and Bothun 2013))

- **Supported Lipid Bilayers (SLBs)**

Supported Lipid bilayers (SLBs) represent models to mimic the lipid bilayer of the biological membrane. SLB consist of a supported smooth lipid bilayer supported on a solid surface such as mica, glass or silicon oxide wafers (Figure 4). They can be used, for example, to study the enzymatic lipolysis or to understand the binding mechanisms of antibacterial drugs, allowing

the investigation of interactions with lipid head groups. Also this model can be used to predict the phase behavior and the molecular lateral organization of biological membranes.

SLB can be prepared by: (I) Langmuir-Blodgett technology, (II) fusion of lipid vesicles or (III) surfactant reduction from micellar solutions collected of a mixture of surfactants and phospholipids.

Furthermore, SLBs models has the advantage to be quick and easy prepared. They present a high stability. It should be noted that its physicochemical properties in terms of lipid composition, leaflet asymmetry, in-plane structure, mobility, and fluidity have been widely considered by techniques like atomic force microscopy (AFM), dissipation-enhanced, ellipsometry, neutron reflection, fluorescence microscopy, and interferometric scattering microscopy (Lind, Cárdenas, and Wacklin 2014) (Deleu et al. 2014).

In addition, another way of obtaining SBLs is through the fusion of small unilamellar vesicles on a hydrophilic substrate. Although a thin layer of water remains between the supported bilayer and its support. The proximity to the support can result in a loss of the lipid degrees of freedom (Bourgau and Couvreur 2014).

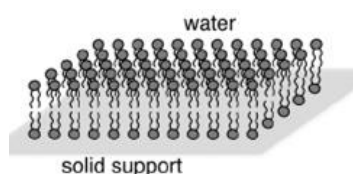


Figure 4 - SLBs as a model to mimic the lipid bilayer of the biological membrane. (Adapted by (Chen and Bothun 2013))

- **Liposomes**

Liposomes are defined as a lipid vesicle in which aqueous compartments are in the core (hydrophilic) or between the lipid bilayers and non-aqueous compartments also exist simply in the phospholipid bilayer (lipophilic), as can be seen in the figure 5 (Kim 2016; Spuch and Navarro 2011). Liposomes are an adaptable mimetic biomembrane model widely used in membrane phase behavioral studies, and processes such as fusion, molecular recognition, cell adhesion, membrane trafficking and pore formation. They are synthetic lipid spheres produced from an aqueous dispersion of membrane lipids (pure or blended) and enfold a small aqueous compartment (Deleu et al. 2014). The liposomes formation is due to the hydrophobic interaction between the phospholipids.

Lipid vesicles more easily demonstrate the complexity of the biological membrane structure once they are arranged in a very similar way to the biological membrane. However, they do not guarantee long-term stability, which is why they are called metastable structures (Deleu et al. 2014; Kim 2016).

Liposomes represent a membrane model widely used in the characterization and investigation of lipid interactions in nanosystems, owing to their exclusive characteristics specifically their capacity to incorporate hydrophilic and hydrophobic drugs. These advantages can be explained based on its composition since it is based on natural substances (Spuch and Navarro 2011; Mufamadi et al. 2016; Caracciolo and Amenitsch 2012). Furthermore, they are widely used to estimate drug efficacy, explicitly to determine the partition coefficient by measuring the amount of molecules incoming into or through the biological membrane (Rodrigues et al. 2001). Previously studies also demonstrated the possibility of understanding the toxicity of some drugs in these models (Baciu et al. 2006; Baginski, Czub, and Sternal 2006).

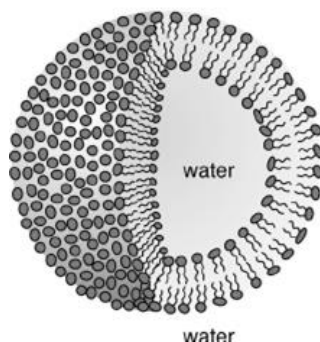


Figure 5 - Liposome as a lipid vesicle with the core hydrophilic cover by the lipid bilayers (lipophilic). (Adapted by (Chen and Bothun 2013))

Drugs on Alzheimer's disease treatment

The pharmacological therapies studied until the date has been in the sense of slowing the progression of AD and alleviate the symptoms. Some drugs already approved for this pathology include cholinesterase inhibitors donepezil hydrochloride (donepezil), galantamine hydrochloride (galantamine), rivastigmine tartrate (rivastigmine), tacrine hydrochloride (tacrine) and memantine, an N-methyl-D-aspartate (NMDA) receptor antagonist. Furthermore, drugs such as statins, clioquinol, and certain nonsteroidal anti-inflammatory drugs have been used (Nussbaum, Seward, and Bloom 2013). However, the benefits are modest (Hansen et al. 2008).

Thus, the use of membrane models for the study of interaction with several molecules has been widely used. Namely, with peptides such as cell penetrating peptides (CPPs),

antimicrobial peptides (AMPs), viral fusion peptides, lipopeptides or amphiphilic pharmacological drugs (Seddon et al. 2009; Peetla, Stine, and Labhasetwar 2009). With this and through biophysical approaches a better understanding of the interaction liposomes-drug is very important for the pharmacological science (Deleu et al. 2014).

Drugs to cross the BBB

The barriers that protect the CNS are extremely strict in controlling the substances that enter the brain. Various studies have been developed in order to increase the amount and concentration of therapeutic compounds in the brain (Gabathuler 2010). The conditions for penetration that can occur are achieved through correct balance of permeability, a low potential for active efflux and the suitable physicochemical properties that permit drug partitioning and distribution into brain tissue (Jeffrey and Summerfield 2010). The capacity of the passage through BBB also depends on molecular size, which should be less than 500 Daltons, low hydrogen bonding capacity, and high lipophilicity. Therefore, one of the pharmacological approaches to overcome this fact is the modification of molecules with previous knowledge that from the outset they penetrate the BBB. Modification can occur through the reduction of polar groups thereby increasing drug transfer. Once more, due to unique physicochemical characteristics of liposomes, they are capable to incorporate hydrophilic and hydrophobic therapeutic agents as is shown in figure 6 (Vieira and Gamarra 2016).

Through a physiological approach the most effective way to cross the BBB will be through specific transporters or internalization of receptors in the neuronal capillaries. Drugs may further be altered to take advantage of carriers specific for the nutrients crossing through the BBB or by conjugation with ligands which recognize the receptors expressed in the BBB (Gabathuler 2010).

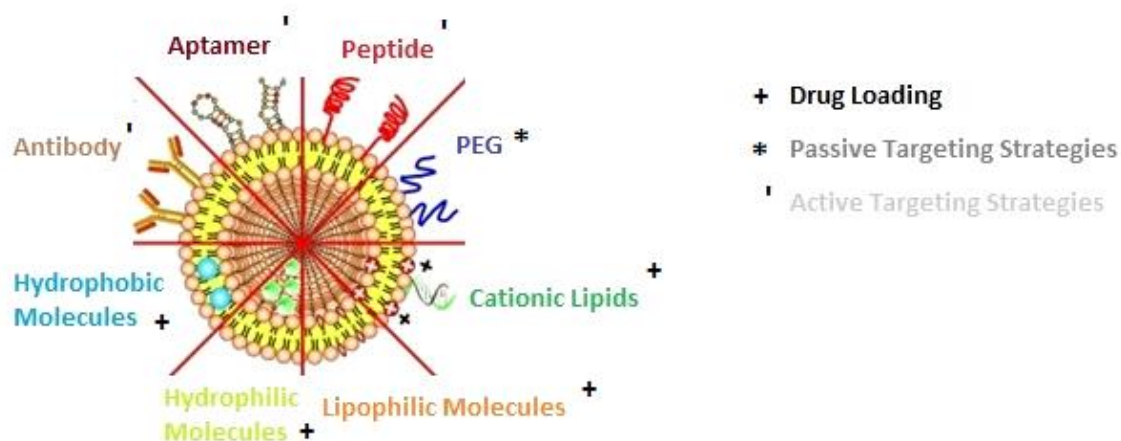


Figure 6 - Schematic representation of the main liposomal drugs and targeting agents that improve liposome affinity and selectivity for brain delivery. Adapted by (Vieira and Gamarra 2016)

Fluorinated Compounds

For the development of new drugs, there was a significant impact of products of natural source and small molecular sizes (Purser et al. 2008). Fluorine is characterized by being an atom of small dimensions and with a very high electronegativity. Its covalent bond is less than a methyl or amine group, but greater than hydrogen having a Van der Waals radius of 1.47 Å. It is interesting to ask why 20 to 25% of the drugs contain in their structure a fluorine atom, since the organofluorinated compounds are practically absent from natural compounds. In 1957 the first synthetic fluorine drug, the antineoplastic agent 5-fluorouracil, was synthesized for the first time, demonstrating high anticancer activity by inhibition of a specific enzyme. Since then, fluorine substitution has been increasingly used in chemical medicine for demonstrating improvements in metabolic stability, bioavailability and protein-ligand interactions. (Purser et al. 2008). An intense flow of fluorine compounds in the pharmaceutical industry has brought immense advances, including steroidal and nonsteroidal anti-inflammatory, central nervous system drugs, anticancer agents and antiviral agents.

At low concentrations, fluorinated solvents like trifluoroethanol and hexafluoroisopropanol demonstrated capacity to stabilize the structure of A β monomers (Rocha et al. 2008). Other studies have also shown that these organofluorinated compounds have already been studied in relation to protein misfolding (Török et al. 2006).

Thus, recent strategies for the introduction of fluorine atoms focus on the following:

- To determine the bioavailability of a compound, a key factor is the metabolic stability. Hepatic enzymes, with their rapid oxidative metabolism, in particular cytochromes, are often found to limit bioavailability. To overcome this problem, a blockage of the reactive site is often accomplished by the introduction of a fluorine atom.
- The basicity of a compound can also be altered because of the fluorine atom. Highly basic groups may reveal a limiting effect on bioavailability. A fluorine atom introduced near a basic group decrease its basicity, which results in a better membrane permeability of a compound and consequently improves bioavailability.
- Yet, it is increasingly common for fluorine substituent to be introduced in order to increase the binding affinity of a compound (Böhm et al. 2004).

So, a very important fact is that it has been proved that organofluorinated compounds with highly negative zeta potential and hydrophobic fluorinated core have the fundamental characteristics to prevent A β fibrillogenesis (Rocha et al. 2008).

Peptides for Alzheimer Disease

As previously mentioned substances that bind to the A β peptide and influence its aggregation are of particular interest. In addition to existing small drug molecules, peptides, linear molecules with (< 100) amino acid residues, have emerged as an interesting therapy as an alternative to chemical pharmaceuticals. The market for these peptides has been increasing since they demonstrate characteristics such as the regulation of biological functions; they offer high biological activity, high specificity and low toxicity. Lately, large libraries of synthetic peptides have been established, with 67 peptides currently on the market, with 150 still in the clinical phase and 400 in the pre-clinic. However, despite this progress several obstacles arise due to their short life, which leads to easy degradation by proteases and problems related with delivery and administration. On the other hand, these problems can be overcome since the chemistry of the peptide allows their modification. In this way they provide a class of reagents that help to understand the mechanism of amyloid aggregation. Thus, a wide range of peptides binding to A β that block amyloid formation has been widely investigated (Aileen Funke and Willbold 2012).

Peptides that were revealed to be effective in rodent AD models or in clinical studies are shown in table 2.

Table 2 - AD Therapeutic Peptides: The Peptide Category, Name, Sequence, Description and Related References.

Peptide Category	Name	Sequence	Description	References
A β -sequence derived β -sheet breaker	iA β 5	LPFFD	Proline based β -sheet breaker	(Soto et al. 1996)
	Ac-iA β 5-amid	Ac-LPFFD-amid	iA β 5 derivatives to improve pharmaceutical properties	(Chacon et al. 2004)
	LPYFD-amid	LPYFD-amid		(Szegedi et al. 2005)
Dipeptide β -sheet breaker	NH ₂ -D-Trp-Aib-OH	Ac-Trp-Aib	β -sheet breaker	(Frydman-Marom et al. 2011)
A β -ApoE4 interaction blocker	A β 12-28P	Ac-VHHQKLPPFAEDVGSNK-amid	A β -sequence derived	(Sadowski et al. 2004)
Anti-inflammation and oxidative stress compound	D-4F	Ac-DWFKAFYDKVAEKFEAF-NH ₂	Apo A-I mimetic peptide	(Handattu et al. 2009)
Selected with combinatorial peptide libraries	D3	RPRTLHTHRNR	Mirror image phage display of combinatorial peptide libraries	(Sun, Funke, and Willbold 2012)

Therefore, in the present study, were tested two different peptides that could inhibit the early stages of A β aggregation.

The sequence LP β FFD was previously developed by Loureiro et al. (2014), based on the 17 to 21 hydrophobic core of A β that can binds to the full length A β preventing its aggregation. The amino acid Pro was coupled with a fluorine atom. Moreover, PEG was added since its toxicity is low, and it is known to reduce proteolytic degradation and increase the solubility of the compounds (Loureiro et al. 2014). By analyzing the amino acids individually, the Phe being hydrophobic and aromatic has a higher A β -binding capacity, which may also be due to steric immobilization by the aromatic ring (Wu et al. 2009). Leu is characterized by their hydrophobic side chains, whereas Asp is an amino acid charged with a carboxyl group on the side chain, negatively charged when it is at the C-terminus, which gives it some hydrophilicity (Santoso et al. 2002). Pro discloses potential chemical inhibition against A β fibrillogenesis, since it has been recognized in previous studies as an amino acid with specific recognition and binding to A β fibrils, since belongs to the class of charged amino acids. (Török et al. 2006; Aileen Funke and Willbold 2012)

The second peptide sequence used in this work has six amino acids, and it is specific to inhibit the amyloid- β peptide. Therefore, it is a still confidential sequence and for this reason,

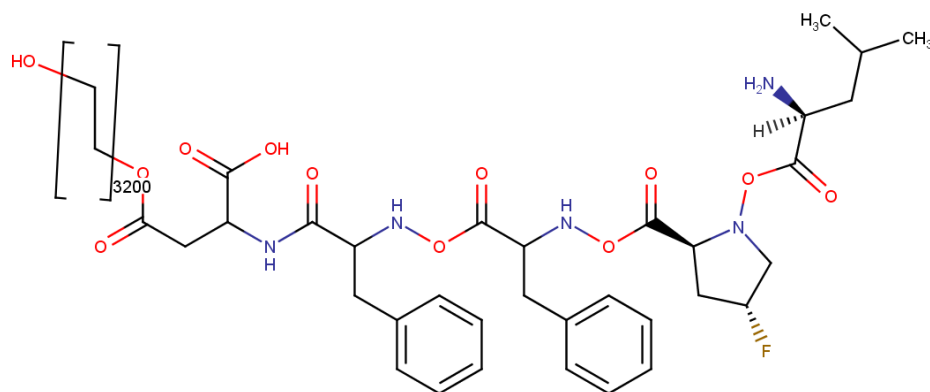
the name will be presented by A β PepInib. It is known that high hydrophobicity peptides are expected to have no difficulty in cross the BBB (Aileen Funke and Willbold 2012). Still, it is of relevant interest to synthesize peptides whose size is small to correspond to a self-recognition of the native amyloid sequence, thereby facilitating binding (De Bona et al. 2009).

Chapter 3

MATERIALS AND METHODS

Materials

A β Peplnib was obtained from GenScript® (Piscataway, NJ, USA) with a purity higher than 96.4% and a molecular weight of 855.02 g/mol. Peptide LP β FFD-PEG (Leu-FluoroPro-Phe-Phe-Asp-PEG) was used as previously described in Loureiro *et al.* (2014) (Figure 7). 1,2-dimyristoyl-*sn*-glycero-3-phosphocholine (DMPC) and Chol (ovine wool; purity > 98%) were purchased from Avanti Polar Lipids, Inc. (Alabama, USA). The fluorescent probe 1,6-diphenyl-1,3,5-hexatriene (DPH; purity > 98%) was obtained from Sigma-Aldrich (Aldrich, Stemheim, Germany) and was prepared by dissolving in chloroform/methanol (3:1, v/v) (Table 3). Peptides solutions and lipid suspensions were prepared with phosphate buffered saline (PBS buffer) pH 7.4 (10 mM PBS, 2.7 mM potassium chloride and 137 mM sodium chloride, Sigma-Aldrich). The buffer was previously prepared with ultrapure water purified with Mili-Q equipment with the specific resistance of 18.2 M Ω ·cm (Milli-Q Academic, Millipore, France) and filtered before use with a membrane filter (0.22 μ m pore size, Restek, Bellefonte, EUA). The β -amyloid (1-42) human (> 99.8%) was purchased from GenScript® (Piscataway, NJ, USA). A β ₍₁₋₄₂₎ was pretreated with HFIP (1,1,1,3,3,3-hexafluoro-2-propanol) (\geq 99.8%) purchased from Sigma-Aldrich. DMSO (dimethyl sulfoxide for molecular biology, \geq 99.9%) was purchased from Sigma-Aldrich. For the grids preparation for morphological TEM analysis, uranyl acetate was used (Electron Microscopy Sciences, Hatfield, PA, USA).

Figure 7 - Chemical Structure of LP₇FFD-PEG peptide. (Marvin Software)

Methods

1. Mass Spectrometry

The time-of-flight (TOF) mass spectrometer (MS) is the method that allows nonscanning mass analyzer through pulses of ions from the source, in seconds. The ions are accelerated so that they have equal kinetic energy before entering the field of the flight tube. Through equation 1, where m is the mass of the ion and v is the ion velocity, the lower the ion mass, the greater the velocity and the shorter its flight time. The time travel from the ion source through the flight tube to the detector is given by m/z value. Because all ion masses are measured for each transient, TOF mass spectrometers are well-suited for the analysis of both targeted and nontargeted analytes. TOF-MS system, being a non-scale instrument, has many advantages such as fast acquisition rates, spectral continuity, and exceptional dynamic range. Through the total mass spectrum it is possible to carry out both qualitative and quantitative analyzes over a wide range with complex matrices (Binkley and Libarondi 2010; Li et al. 1999).

$$E = \frac{1}{2}mv^2 \quad (1)$$

For this technique was used positive electrospray ionization mode (ES +) since it allows a greater degree of ion fragmentation (Chan et al. 2007).

2. Transmission Electron Microscopy (TEM)

A powerful and distinctive technique to the structural characterization of the material surface commonly used is transmission electron microscopy (TEM). TEM allows visualization of the distribution of atoms in *nanostructures*. It includes an illumination system, a specimen stage, an objective lens system, the magnification system, the data recording system, and the chemical analysis system (figure 8). This technique allows the visualization of images with atomic resolution of 1 nm. TEM consists of a finely focused electron probe that allows the electronic characterization of the nanoparticles individually (Wang 2000).

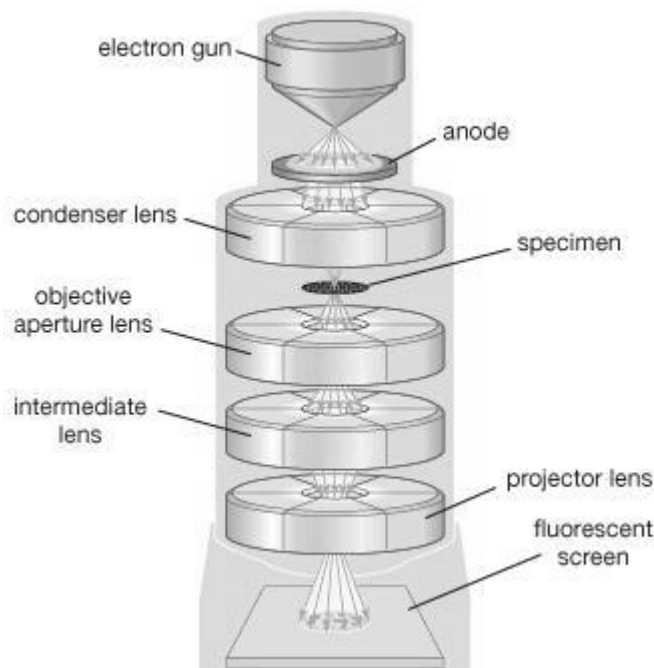


Figure 8 - Principle of transmission electron microscopy (Adapted by Enciclopedia Britannica, Inc.)

$A\beta_{(1-42)}$ was incubated at 37 °C, alone and in the presence of the $A\beta$ Peplnib peptide (1200 μ M). The samples were incubated for 24 hours, with gentle agitation and with an $A\beta$ final concentration of 30 μ M. Samples in the absence of $A\beta_{(1-42)}$ were also run at the same experimental conditions. Aliquots of 5 μ L of each sample were placed on carbon-formvar coated 200-400 mesh spacing grids and let to adsorb for five minutes. Grids were washed with 2% filtered uranyl acetate solution once and negatively stained with the same solution for 45 seconds. The visualization of the grids was done by a Jeol JEM 1400 electron microscope at 80 kV.

3. Liposomes Preparation

Liposomes were prepared by the lipid film hydration method (Lasic 1997; Dua, Rana, and Bhandari 2012; Popovska 2014).

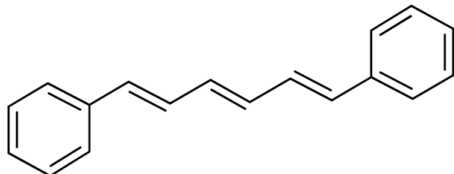
First the lipids are dissolved in chloroform (CF), forming a homogeneous lipidic mixture. Thereafter, the lipid film, with and without Chol, is formed by evaporation of the chloroform with a stream of nitrogen. The molar ratio was DMPC:Chol [85:15]. This is a critical step, since the complete removal of the organic solvent is required, in a slow mode and with continuous rotational movements. The nitrogen atmosphere allows rapid solvent evaporation and inhibits lipids oxidation. The resulting lipid film was hydrated with PBS buffer 7.4 and the mixture was vortexed (Vortex Genius 3, Ika®, Germany) at temperature above the phase transition temperature of lipid for complete dissolution (approximately 10 minutes), to yield MLVs. (Koynova and Caffrey 1998) The suspension was submitted to ultrasound in a sonicator bath (Ultrasonic cleaner, VWR®, Malaysia) for 10 minutes, followed by extrusion through polycarbonate membranes (Nuclepore Track-Etch Membrane, Whatman®, Maidstone, UK) with a specific size 11 times using an extruder (Mini-extruder, Avanti Polar Lipids, Alabama, USA). The liposomes were then sequentially passed through membranes with pore diameters of 400, 200 and 100 nm.

The size of the LUVs formed was confirmed by dynamic light scattering analysis in a ZetaSizer Nano ZS (Malvern Instruments, Worcesterchire, UK).

For the fluorescence measurements, the probe (DPH) was codissolved with the lipids (DMPC or DMPC:Chol) in the organic solvents mixture to give a probe/lipid molar ratio of 1:100.

Table 3 - Chemical structure of the compounds used to prepare liposomes (by Sigma Aldrich)

Chemical Name	Structure
1,2-dimyristoyl- <i>sn</i> -glycero-3-phosphocholine (DMPC)	
Cholesterol (Ovine Wool)	

1,6-Diphenyl-1,3,5-hexatriene (DPH)	
--	--

4. Liposomes Characterization

The control of physical properties of liposomes is a very important step, and it can be done through measurements such as mean vesicle size, size distribution, electrical surface potential, morphology and surface pH lamellarity. To the naked eye, a variation in composition and size of the liposome suspension can be perceived since the coloration varies from translucent to milky, from lower concentration and size to greater, respectively (Popovska 2014). Usually, to control these properties the DLS technique is commonly used.

4.1. Size and Pdl

Dynamic Light Scattering (DLS), also known as photon correlation spectroscopy, is a widely used technique for nanoparticle (NP) size determination. This technique consists of exposing NP to an electromagnetic wave, the direction and intensity of which are altered due to the scattering phenomenon. As NPs are in constant Brownian motion due to their kinetic energy, intensity variation occurs over time and information about this brownian motion can be used to measure the diffusion coefficient.

For spherical NPs, the hydrodynamic radius of the particle can be calculated from its diffusion coefficient by the Stokes-Einstein equation:

$$D_f = \frac{k_B \cdot T}{6\eta\pi R_H} \quad (2)$$

where k_B is the Boltzmann constant, T is the temperature of the suspension, and η is the viscosity of the surrounding media. R_H is the hydrodynamic radius, corresponding to the radius of a sphere that has the same diffusion coefficient within the same viscous environment of the particles being measured. It is directly related to the diffusive motion of the particles (Lim et al. 2013).

This technique allowed the determination of particle size and dispersion distribution (polydispersity index, Pdl) using a ZetaSizer Nano ZS (Malvern Instruments, Worcesterchire, UK). This index indicates the heterogeneity of the suspension. The suspension is monodisperse when the particles have the same overall size and the Pdl is < 0.1 (Jiang, Oberdörster, and Biswas 2009). All the determinations were performed in disposable cells (Sarstedt, Germany)

and the dispersing medium used was PBS. The measurements were made at 25 °C and both size and Pdl were calculated to the average of 10 runs, in triplicate.

4.2. Zeta Potential

The characterization of the surface charge properties of the nanoparticles can be obtained by measuring the zeta potential (ζ -Potential). A very high value of zeta potential implies very high colloidal stability. It is known that for values of zeta potential above (+/-) 30 mV the suspension is stable (Popovska 2014). This measurement is based on the principle that when a particle in the presence of an electric field moves, the ions present at this boundary move with it. The electric potential at the NP surface is the zeta potential. Thus, in the presence of an induced electric field, it is possible to ascertain the electrophoretic mobility of the particles that progress towards the electrode with opposite charge. Viscous forces will oppose the movement of particles until equilibrium is achieved. The electrophoretic mobility can then be calculated by analyzing the electrophoresis under different experimental conditions. Through the use of Henry's law it is possible to determine the zeta potential of the particle:

$$U_E = \frac{2\epsilon z f(ka)}{3\eta} \quad (3)$$

Where z is the ζ -potential, U_E the electrophoretic mobility and $f(ka)$ the Henry's function (Freire et al. 2011). To measure the ζ -potential of the particles in suspension a ZetaSizer Nano ZS (Malvern Instruments, Worcesterchire, UK) was used. Folded capillary cells from Malvern (Worcesterchire, UK) were used and the dispersant medium was PBS. The zeta potential was obtained by the average of 3 measurements (each one with 12 runs).

5. Determination of Partition Coefficients by Derivative Spectrophotometry

One of the most important physico-chemical properties in the pharmacokinetic and pharmacodynamic profile study of the drugs is the hydrophobicity. The partition coefficient represents the mode of compound distribution in a mixture of two immiscible equilibrium phases, and can be used as a measure of hydrophobicity. This ratio measures the solubility difference of the compound in the phases in equilibrium as well as the concentration of ionized and non-ionized species (Kwon 2001). With the partition coefficient (K_p) determination (equation 4), it is possible to obtain indications on the distribution of drugs between the

aqueous and lipidic phases, and can be used in studies of absorption, distribution, metabolism and elimination of drugs, as well as evaluation of toxicity (Magalhães et al. 2010). Theoretical values of partition coefficients for the tested compounds were calculated from Marvin sketch calculator software from Chemaxon™. This software allows the design and validation of the molecular compound through an integrated nuclear magnetic resonance predictor. It enables a fast and accurate prediction of basic physicochemical properties such as logP, logD and pK_a.

The K_p of peptides between LUVs suspensions of DMPC or DMPC:Chol [85:15] and the aqueous buffered solution was determined by derivative spectrophotometry. The stock solutions of peptides AβPeplnib and LP₁FFD-PEG were prepared in PBS with a concentration of 1000 μM and 45.79 μM, respectively. For the K_p procedures the final concentrations of peptide used were 600 μM for AβPeplnib and 15.26 μM for LP₁FFD-PEG. The LUVs suspension with increasing concentrations of lipids was 0 - 1000 μM and 0 - 500 μM for AβPeplnib and LP₁FFD-PEG, respectively. The final volume was 300 μL per well. The suspensions were incubated in the dark for 30 min and 37 °C, with gentle agitation. As background, the same experience was performed without peptides. The absorption spectra (200-500 nm range) of samples and reference solutions were recorded in a temperature range from 36 °C to 41 °C, in a multidetection microplate reader (Synergy 2, Bio-Tek Instruments). For the mathematical treatment of the results, an already developed calculation procedure was used through K_p calculator (Magalhães et al. 2010), which (i) subtracts each reference spectrum from the correspondent sample spectrum to obtain corrected absorption spectra; (ii) determines the second and third-derivative spectra in order to eliminate the spectral interferences due to light scattered by the lipid vesicles and to enhance the ability to detect minor spectral features and improve the resolution of bands; and (iii) calculates the K_p values by plotting the second- or third- derivative spectra values at wavelengths where the scattering is eliminated versus the lipid concentrations. A nonlinear least-squares regression method is applied by fitting the following equation to the plot, where K_p is the adjustable parameter:

$$D_T = D_w + \frac{(D_M - D_w)K_p[L]V_\phi}{1 + K_p[L]V_\phi} \quad (4)$$

In this equation, D is the second or third-derivative intensity obtained from the absorbance values of peptides: D_T refers to the total amount of peptide, D_w corresponds to peptide distributed in the aqueous phase, and D_m corresponds to peptide distributed on the lipid membrane phase; K_p is the partition coefficient of the peptide in a specific liposome system; [L] is the molar concentration of the lipid; and V_φ is the lipid molar volume of DMPC (0.663 L mol⁻¹), DMPC:Chol [85:15] (0.623 L mol⁻¹); with the molar volume of Chol 0.394 L mol⁻¹.

6. Phase Transition Temperature Studies

Thermotropic lipid phase transitions are interrelated to discontinuities or abnormalities in macroscopic physical properties such as stability, fluidity or permeability of membranes, which is directly related to their phase transition temperature. It is known that near the transition from the gel to crystalline phase the liposomes become highly permeable. Thus, for the rational design of liposomal models it is necessary to know their behavior due to changes in temperature, and consequently in phase transition temperature (Michel et al. 2006; Aileen Funke and Willbold 2012).

The main phase transition temperature of DMPC and DMPC:Chol [85:15] vesicles in the presence of peptides were determined by DLS, as already described by Michel, N. *et al* 2005.

A fixed concentration of DMPC and DMPC:CHOL (10 000 μ M), A β Peplnib (600 μ M) and LP γ FFD-PEG (15.26 μ M) was used and the sample was incubated, with agitation in a closed quartz cuvette at 37 °C during 30 min. Standard solutions were prepared in the same mode in the absence of the peptides.

Measurements were made using a ZetaSizer Nano ZS (Malvern Instruments, Worcesterchire, UK). The position of the detector was at 173° relative to the laser source (backscatter detection). Software was used in *trend* mode that allows multiple measurements and the temperature in the cell was monitored by an external probe. The temperature ranged from 10 to 55 °C with temperature increments of 0.2 °C (equilibration time of 5 min). At each temperature, 6 runs of 8 seconds were performed. The measurements were performed overnight. This stage was repeated two times so as to achieve accurate reproducibility in the intensity of scattered light.

Results were collected as “mean count rate versus temperature” and the data were fitted using the following equation (Boltzmann Regression Curves):

$$y = \frac{A_1 - A_2}{1 + e^{(x - x_0)/\Delta x}} + A_2 \quad (5)$$

With A_1 , the initial y value (initial count rate of lipids in phase 1), A_2 , the final y value (lipids in phase 2), x_0 , the center of the distribution (y value at x_0 being half way between the two limiting values A_1 and A_2 : $y(x_0) = (A_1 + A_2)/2$) and Δx , the width of the slope. For a complete analysis the software ©2017 GraphPad Software, Inc., was used.

7. Membrane location studies by fluorescence quenching

Studies of fluorescence quenching were first applied in the late 1960s. Since then, this technique has proved to be a very useful tool for the study of proteins, membranes or macromolecules assemblies (Eftink 2002). In this process, when the fluorophore is induced by a variety of molecular interactions by the quencher the fluorescence quantum yield decreases. In the case of the formation of a ground state complex, the fluorescence quenching may be static, but it can also be dynamic when collisions between the quencher and the fluorophore occur. In both situations it is necessary contact between the fluorophore and the quencher (Papadopoulou, Green, and Frazier 2005). This method is based on decreasing fluorescence intensity measurements that occurs when a fluorophore (for example a protein) interacts with an external quencher molecule (for example a polyphenol) thereby promoting a rapid destabilization of its excited state. Through this reaction, quencher provides information on the location of the fluorescence groups in the molecular structure (Joye et al. 2015).

Quenching studies, including fluorescence steady-state measurements, were performed by incubating increasing concentrations of A β Peplnib (from 0 to 600 μ M) and LP β FFD-PEG (from 0 to 15.26 μ M) with DPH labeled liposomes with a fixed concentration of DMPC (500 μ M), in phosphate buffer (pH 7.4). Before fluorescent measurements, the resulting suspensions were incubated in the dark for 30 minutes at a physiological temperature of 37 °C. In this way peptides could reach the partition equilibrium between the lipid membranes and the aqueous medium. The determinations were made immediately after incubation. Fluorescence quenching studies were performed in a spectrofluorimeter. All measurements were recorded at 37 °C with excitation/emission wavelengths of 357/427 nm for DPH. Fluorescence emission intensity values were corrected for the inner filter effects at the excitation wavelength.

The aptitude of both peptides to quench the fluorescence of DPH probe was evaluated by determination of the slope of the Stern–Volmer plots obtained by steady-state fluorescence measurements (I_0/I) versus the quencher concentration ($[Q]$) (Neves et al. 2016).

$$\frac{I_0}{I} = 1 + K_{SV}[Q] \quad (6)$$

where I and I_0 are the fluorescence steady state intensities with and without the quencher, respectively, K_{SV} is the Stern Volmer constant and $[Q]$ is the membrane effective concentration of peptides, which is calculated from the total drug concentration ($[Q]_T$) and from drug's partition coefficient (K_p), as described in following equation:

$$[Q] = \frac{K_p[Q]_T}{K_p\alpha_m + (1-\alpha_m)} \quad (7)$$

where α_m is the volume fraction of membrane phase ($\alpha_m = V_m/V_T$; V_m and V_T represents, respectively, the volumes of the membrane and water phases).

Chapter 4

RESULTS AND DISCUSSION

Peptide Characterization

Since the A β PepInib sequence is confidential, the real molecular mass of A β PepInib was quantified by TOF-MS in order to compare with the theoretical one.

As can be seen in figure 9, there are several formed peaks resulting from peptide fragmentation. The last peak observed corresponds to the peptide protonated form $[M + H]^+$, consistent with the donation of an electron thus having the result of the entire molecular mass of the compound. The remaining peaks correspond to fragmented, protonated and deprotonated forms that can be originated through carboxylic groups.

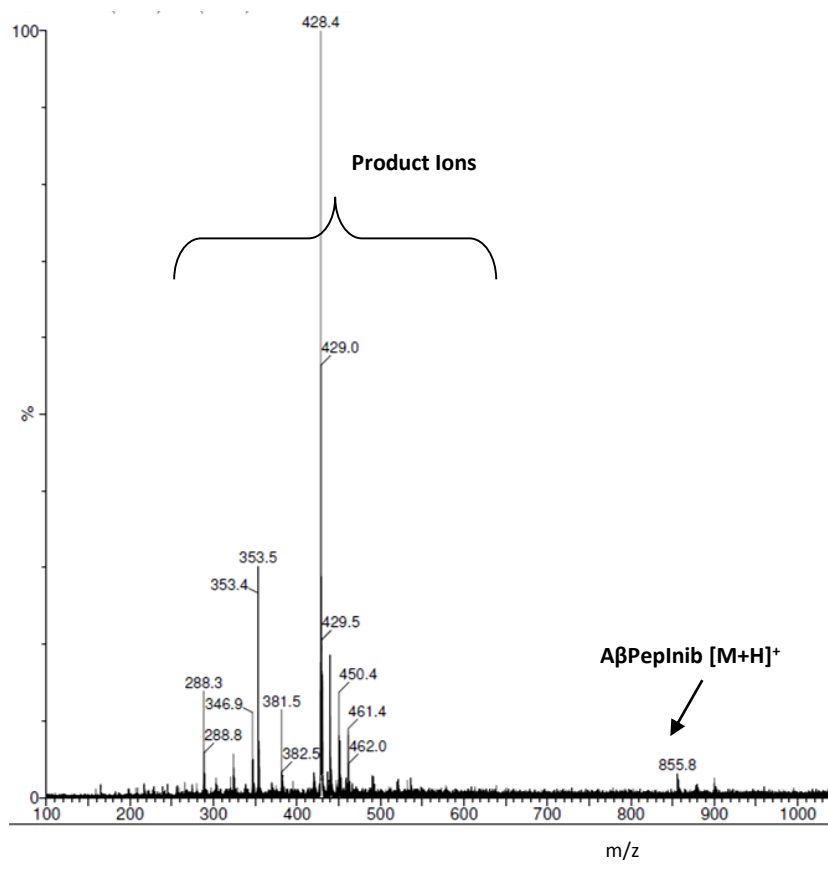


Figure 9 - TOF MS of the A β PepInib peptide

The value of 855.8 Da is consistent with the theoretical value of 855.02 Da, thus confirming the sequence of the peptide under study.

Structural Analysis of Amyloid beta Peptide

TEM was used to the morphological analysis of fibril formation of the $A\beta_{(1-42)}$ peptide alone and in the presence of the new peptide $A\beta$ PeptInib. The $A\beta_{(1-42)}$ in absence of $A\beta$ PeptInib was observed as a control. The results are shown in figure 10.

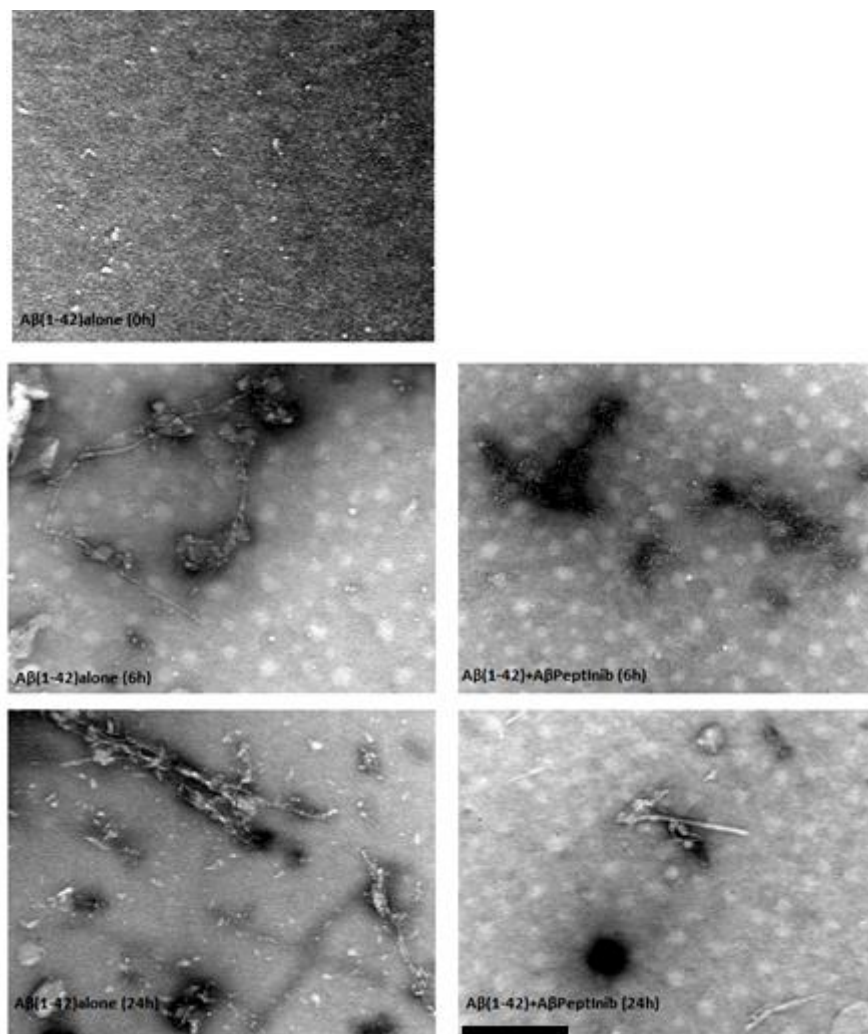


Figure 10- Transmission Electron Microscopy images of the effect of $A\beta$ PeptInib peptide on the $A\beta_{(1-42)}$ aggregation. The samples were incubated for 24 hours, and the figure present 3 time points: 0 h, 6 h and 24 h. The scale bar correspond to 100 nm.

TEM analysis showed that $A\beta_{(1-42)}$ incubated at 37 °C for 24 hours resulted in amyloid-like unbranched fibrils. At 6 hours $A\beta$ incubated with both peptides only presents amorphous aggregates and small fibers. On the other way, after 24 hours incubation the formation of

fibers occurs, however a decrease of its intensity is verified when compared with A β alone. This analysis demonstrates that the A β PepInib delays the A β ₍₁₋₄₂₎ fibrillogenesis.

Liposomes Characterization

Liposomes were produced by the technique of hydration film and then were characterized in terms of size and charge. From table 4 it is possible to see for DMPC liposomes the mean diameter is 129 ± 1 nm and for DMPC:Chol 143 ± 2 nm. The Pdl of both suspensions were less than 0.1, which suggests the homogeneity of the dispersion. It is found that the zeta potential is slightly negative, conferred by the slight negative charge of the DMPC, which indicates the stability of the prepared suspension for both DMPC alone and DMPC with Chol. Moreover, the values of ζ -potential are close to 0 once that DMPC is a neutral lipid (table 3). As described in Magarkar et al. (2014), the presence of chol will decrease Na⁺ ion binding with the lipid headgroup, as a result the surface charge becomes more neutral as can be seen in table 4.

Table 4 - Mean diameter, PDI and Zeta Potential of the liposomes with and without cholesterol (n=3;*n=2)

	Mean Diameter (nm)	PdI	Zeta Potential (mV)*
DMPC	129 ± 1	0.07 ± 0.02	-4 ± 3
DMPC + CHOL	143 ± 2	0.041 ± 0.009	-2.9 ± 0.9

Determination of Partition Coefficient by Derivative Spectrophotometry

The interactions of A β PepInib and LP γ FFD-PEG with the membrane model system were studied from the determination of the partition coefficients (K_p). The system used was liposomes-water instead of the common octanol-water system, thus providing an environment that better simulates the cell membrane. Also, it is possible in this way to take into account not only the hydrophobic interactions, but also electrostatic and hydrogen bond interactions.

Thus, the K_p determination, which then provides information on the distribution of drugs between aqueous and lipidic phases, without the need to quantify the drug separately in each media, facilitates an understanding of the process of passive diffusion through the

biological barrier. K_p was evaluated by derivative spectrophotometry. The background signals of liposome light scattering were eliminated, providing a better resolution of overlapped bands. K_p assays are based on the changes in spectral characteristics of peptides when it permeates from the aqueous to the lipid phase (Lúcio et al. 2009; Neves et al. 2016).

Figure 11 illustrates the absorption spectra of A β Peplnib with increasing concentrations of LUVs of DMPC (gray lines) at pH 7.4 and 37 °C. The absorption spectrum cannot be used directly due to the high background produced by the lipid/drug interactions that induce false K_p values. In figure 11 (right) the respective second-derived spectra is also presented. It is possible to verify that the effect of background signals is eliminated (gray lines), and the resolution of the signal is significantly improved by sharpening them (black lines). For the LP ϵ FFD-PEG peptide the third derivative spectra was used (figure 12, right). As can be seen the effect of the background elimination and the increase in resolution is quite significant which provides a better determination of K_p and interpretation of the spectra.

Moreover, it is possible to perceive a slight and discrete shift in λ_{max} with increasing lipid concentration in both peptides, which gives a somewhat clearer indication that the drug partitions from the aqueous to lipid media.

K_p values were obtained using the nonlinear least square regression method (Magalhães et al. 2010), by fitting equation 4 to experimental second-derivative spectrophotometric data (D_t vs. $[L]$). The wavelengths (where the scattering is eliminated) used, were 272 nm for A β Peplnib (Figure 11) and 256 nm for LP ϵ FFD-PEG (Figure 12).

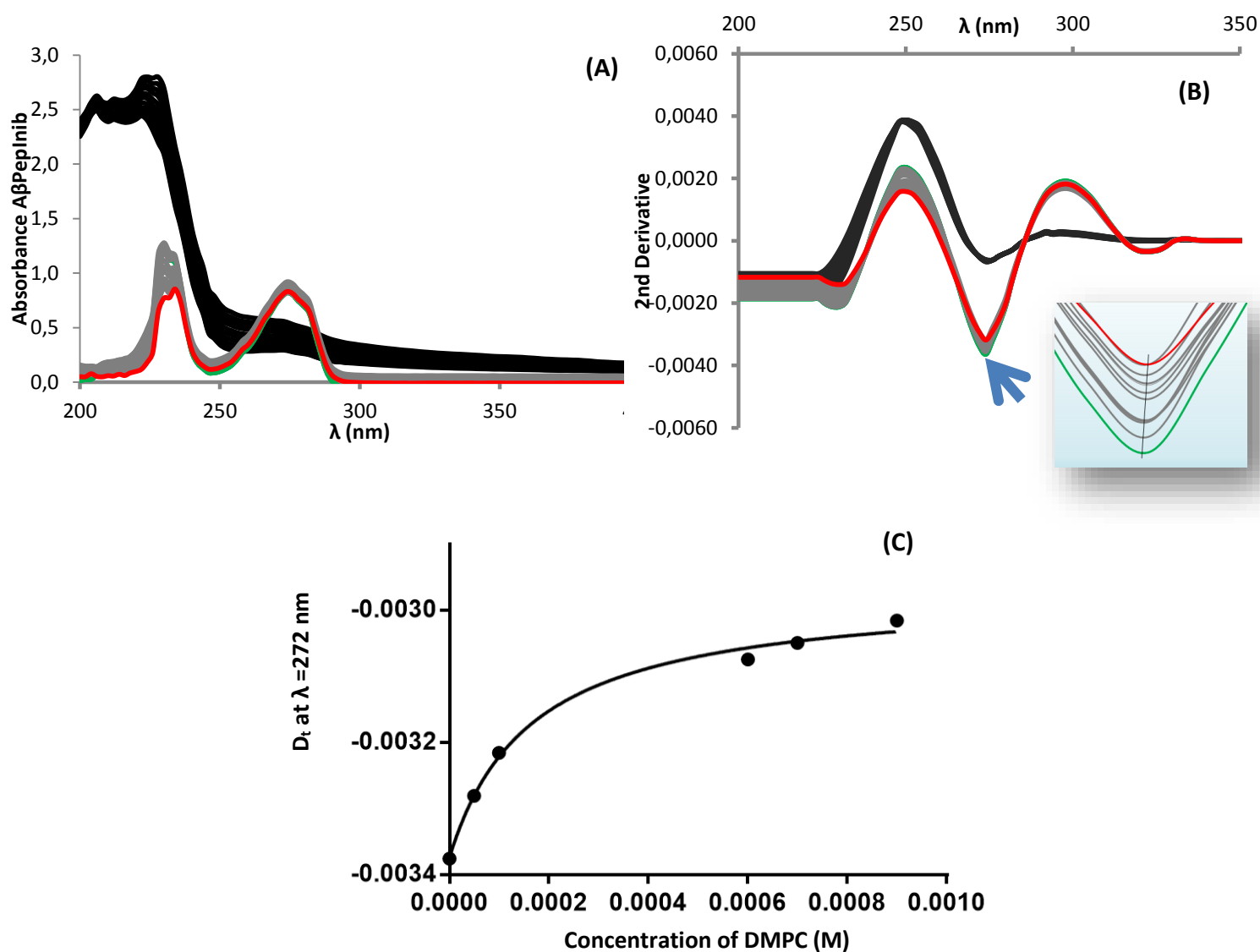
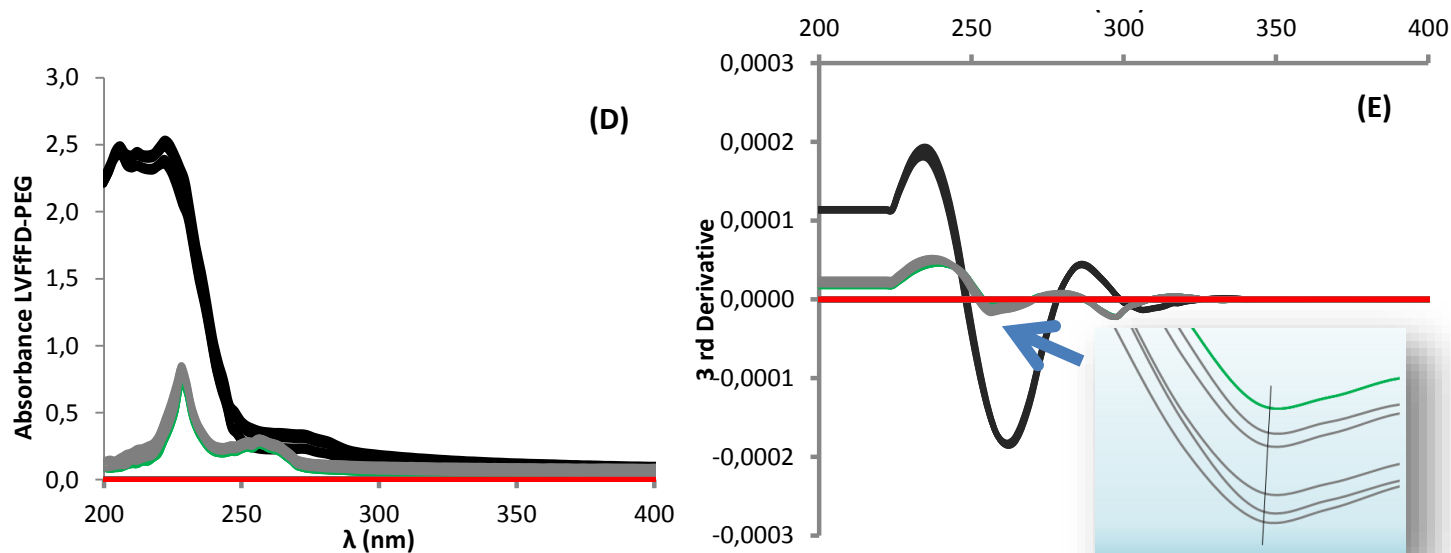


Figure 11 - Absorption spectra (A) and second-derivative spectra (B) of AβPeplinib (600 μM) incubated in LUVs of DMPC at 37 °C (gray lines) and LUVs of DMPC without drug (black lines) at increasing lipid concentrations (n=3). The curve C represents the best fit by Eq. (4)



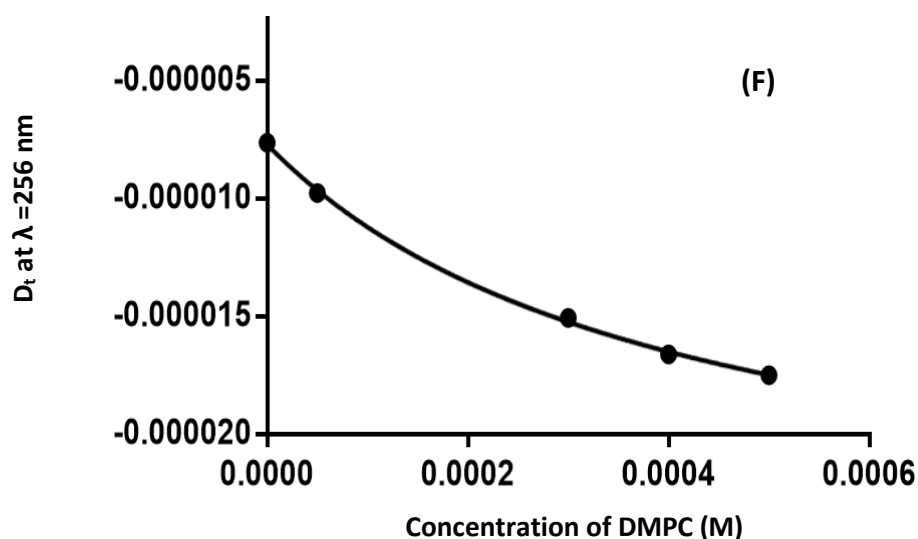


Figure 12 - Absorption spectra (D) and third-derivative spectra (E) of LPfFFD-PEG (15.26 μ M) incubated in LUVs of DMPC at 37 °C (gray lines) and LUVs of DMPC without drug (black lines) at increasing lipid concentrations. The curve F represents the best fit by Eq. (4) ($n=2$)

The liposomes aqueous partition coefficients of both peptides were determined at six different temperatures (from 36 to 41 °C, with 1°C increments) for the two distinct systems, DMPC alone and DMPC:Chol [85:15]. The values of K_p obtained for A β PepInib are listed in table 5 and for LPfFFD-PEG in table 6.

Table 5 – Partition coefficients values obtained for A β PepInib expressed as K_p and logD ($n=3$; $*n=2$)

System	T (°C)	$K_p/10^3$	LogD
A β PepInib DMPC	36	9.2 ± 2.9	4.0 ± 0.1
	37	6.8 ± 2.7	3.8 ± 0.2
	38	8.6 ± 1.6	3.9 ± 0.1
	39	9.2 ± 1.8	4.0 ± 0.1
	40	8.5 ± 2.1	4.0 ± 0.1
	41	6.8 ± 3.3	4.0 ± 0.2
A β PepInib* DMPC CHOL	36	2.8 ± 1.0	3.4 ± 0.2
	37	2.8 ± 0.3	3.55 ± 0.05
	38	2.0 ± 0.8	3.3 ± 0.2
	39	2.6 ± 0.8	3.4 ± 0.1
	40	2.2 ± 0.5	3.3 ± 0.1
	41	2.8 ± 0.2	3.45 ± 0.03

Table 6 - Partition coefficients values obtained for LP_rFFD-PEG expressed as K_p and logD (n=2)

System	T (°C)	K _p /10 ³	LogD
LP_rFFD-PEG DMPC	36	0.9 ± 0.4	3.0 ± 0.2
	37	2.5 ± 1.7	3.4 ± 0.3
	38	1.3 ± 1.1	3.0 ± 0.3
	39	1.6 ± 0.7	3.2 ± 0.2
	40	1.3 ± 0.4	3.1 ± 0.1
	41	0.6 ± 0.5	2.7 ± 0.3
LP_rFFD-PEG DMPC CHOL	36	2.7 ± 1.1	3.4 ± 0.2
	37	2.9 ± 2.4	3.4 ± 0.4
	38	1.6 ± 0.3	3.2 ± 0.1
	39	3.8 ± 1.7	3.6 ± 0.2
	40	2.6 ± 1.2	3.4 ± 0.2
	41	2.7 ± 1.1	3.4 ± 0.2

The K_p values obtained indicate that the affinity of the AβPepInib:DMPC system to the membrane is higher than the affinity of LP_rFFD-PEG:DMPC to the hydrophobic region. This was observed for all temperatures. The same tendency is observed for the DMPC:Chol system. These results suggest that from drug to drug the partition coefficient between the membrane phase and the aqueous phase is different. The distribution will depend on several properties, such as its structure, degree of ionization and even the molecular packing of the lipids. Moreover, for AβPepInib and all temperatures, the partition of DMPC system is greater than DMPC:Chol system, since the lipids are much more organized and packed in the presence of cholesterol, making more difficult the penetration by diffusion of drugs inside membrane. For LP_rFFD-PEG the difference of values between systems was not noteworthy.

It was not possible to predict the macro species distribution for AβPepInib using the Marvin sketch calculator software. The software does not allow the determination of the majority ionized form represented by macromolecules. However, the pI predicted by the software, (9.1), is above the physiological pH, which indicates that the peptide will be mostly in the cationic form. The partition of the positively charged of AβPepInib can lead to a neutralization of membrane charge by electrostatic attraction with the negatively charged phosphate of the headgroup region of the bilayer, while nonpolar portion inserts and orientate into the hydrophobic core. The predicted value of logP for AβPepInib by Marvin software was -5.14 which is considerable lower than experimental logD. The different types of interactions evaluated by each method justify this discrepancy. The software, which use octanol:water

partition data as reference, mainly considers the hydrophobic interactions, not taking into account the ionic interactions established between charged drugs and phospholipids of the membranes. Thus, this result (Table 5) indicates that A β PepInib should preferentially interact by electrostatic forces.

The pK_a , pI values and octanol/water partition coefficient of LP β FFD-PEG were also determined using the Marvin sketch calculator software. In this case, at pH 7.4, anionic species predominate but a significant contribution of zwitterionic species are also present ($\approx 30\%$). The calculated pI (4.28) of this peptide is also lower than the physiological pH confirming once more the presence of negative charges. The negative charged part of the peptide interacts with the phospholipid head groups with the positively charged choline due to ammonium group explaining the experimental value of $\log D$ for LP β FFD-PEG. The discrepancy between $\log D$ and $\log P$ (-2.97) confirms that not only hydrophobic interactions are present, and that electrostatic interactions should also play a role. These results also underline the high limitation of conventional models to predict the theoretical $\log P$, based on the octanol/water system, since it only takes into account the hydrophobic interactions (Pinheiro et al. 2013). Since both peptides interact with the liposomes by electrostatic forces, it makes sense that the experimental values of both are so close.

Phase Transition Temperature Studies

In the analysis of the biophysical properties of the membrane, the study of phase transition (T_m) of lipids, from gel phase to fluid phase, is of paramount importance. This occurrence of phase transition in lipids reveals a significant impact on membrane fluidity and depends on various factors such as temperature, hydration and lipid composition. For the determination of the lipid transition temperature the technique used was DLS. This technique reflects changes in the optical properties of lipids during temperature variations and is based on measurements of the average count rate (average number of photons scattered detected per second) by DLS instrument (Michel et al. 2006).

Figure 13 shows the influence of peptides on the normalized mean count rate as a function of temperature, in the lipid model system at pH 7.4.

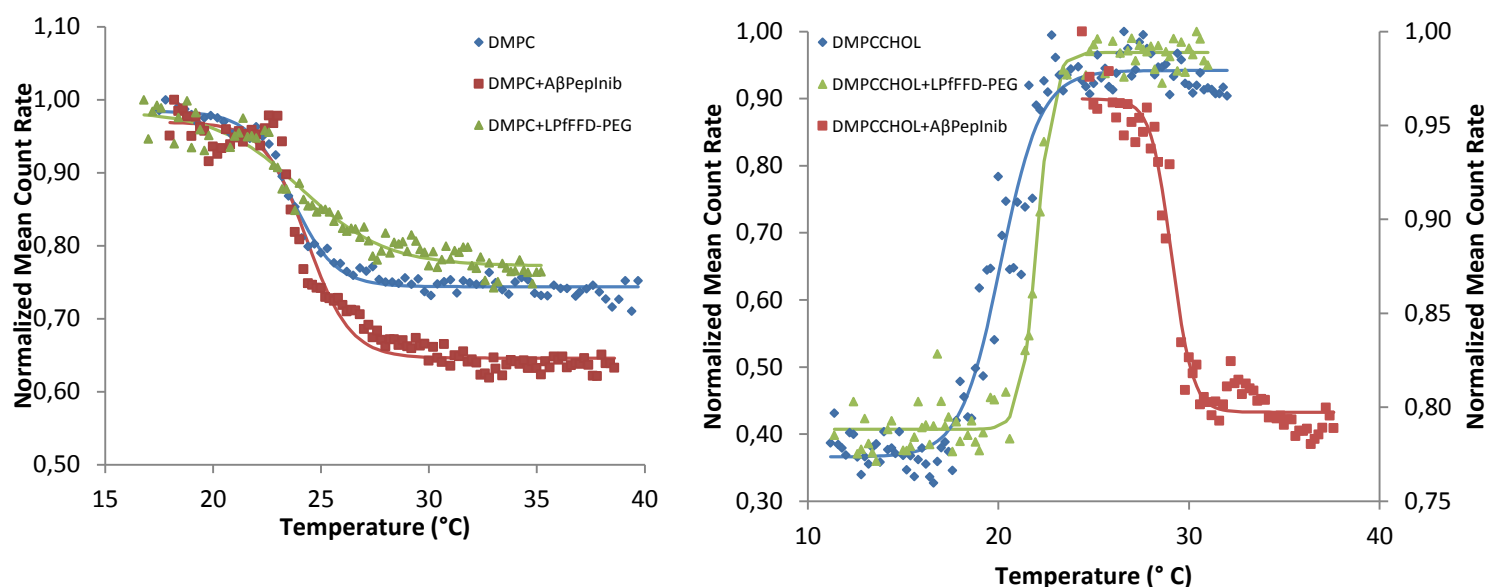


Figure 13 - Normalized mean count rate of DMPC and DMPC:Peptide (left) and DMPC:Chol and DMPC:Chol:Peptide (right) at pH 7.4 as function of temperature.

From the sigmoidal inflection point of the experimental data, it was possible to calculate the T_m of all systems through equation 5. The results obtained for the systems studied are present in table 7.

Table 7 - Values of main phase transition temperature (T_m) obtained from DMPC, DMPC:Chol at pH 7.4 in the absence and presence of peptides, obtained by fitting eq 5. (n=3; *n=2)

	T_m (°C)	R^2
DMPC	24.0 ± 0.3	0.982
DMPC + AβPepInib	24.6 ± 0.3	0.975
DMPC + LP₇FFD-PEG*	24.2 ± 0.1	0.958
DMPC:CHOL	20.3 ± 0.2	0.968
DMPC:CHOL + AβPepInib*	29.06 ± 0.04	0.965
DMPC:CHOL+LP₇FFD-PEG*	22.3 ± 0.3	0.992

The phase transition is based on the disorder of the hydrophobic chains of the lipids. This disorder is preceded by a slight increase in lateral mobility. The headgroups of lipid molecules also have an effect on the lipid phase transition temperature due to electrostatic dipolar interactions (Krause et al. 2014; Alessandrini and Facci 2014). With the analyses of table 7, it can be firstly observed that the phase transition value for pure DMPC (24.0 °C) is

consistent with literature data (Taly, Baciou, and Sebban 2002). The T_m of the pure DMPC raised slightly in the presence of both peptides, about 0.6 for A β Peplnib and 0.2 for LP γ FFD-PEG (table 7) (figure 13 (left)). These alterations demonstrate the disturbing effect of peptides on membrane order. The quantitative differences in T_m of the lipids are due to the location of the molecules in different regions of the lipid bilayer, because in the deepest regions of the bilayer (corresponding to the acyl chains of C9 to C14) the order is smaller than in the superficial regions corresponding to the head of the phospholipids (C1 to C8 acyl chains). Thus, the region where the foreign substances have a minor effect is in the less ordered region, since their fluid nature accommodates them better (Pinheiro et al. 2013). This result is not in agreement with the fact that the electrostatic interactions are predominant, however it can be justified by several factors that affect the phase transition temperature beyond the ionic interactions like the hydrostatic and lateral pressure of the phospholipids or the presence of specific ions (Alessandrini and Facci 2014). It is still possible to observe, once again, the similar behavior between the peptides and the membrane model.

Due to the presence of Chol, the DMPC:Chol system, the membrane is more complex and more organized, and mimics better the cell membrane. However, the presence of a single component in the phospholipid bilayer further promotes lateral heterogeneity. Such heterogeneity may result in very distinct phenomena such as immiscibility and preferential interactions between molecules (Engberg et al. 2015). This particular effect led to the creation of a new phase called liquid-ordered (Lo) phase that increases lateral packing density. Additionally this effect can also affect the bilayer thickness through the elongation of the acyl chains. For the study of phase transition it is known that chol introduces a great complexity (Alessandrini and Facci 2014). By the analysis of the figure 13 and the table 7 it is perceptible that in both situations the peptides interacted with the membrane system raising the transition temperature in relation to the pure system (DMPC:Chol). This increase was about 9 °C for A β Peplnib and about 2 °C for the LP γ FFD-PEG. Relatively to the DMPC:peptide system a different effect was observed. For the A β Peplnib an increase of the phase transition temperature to 29.1 °C was observed whereas for the LP γ FFD-PEG a reduction of the temperature to 22.3 °C was verified. This disparity can also be graphically observed. The mean count rate of NP increases for the pure system and for the LP γ FFD-PEG (Figure 13 right) while the mean count rate of NP for the A β Peplnib system decreases (Figure 13 right). These results show that both peptides have the ability to interact with the membrane, however with distinct interactions. This may occur because the phase transition can often be affected by pH (related to surface charge), ionic strength of the solution, hydrostatic and lateral pressure and the presence of specific ions (Alessandrini and Facci 2014). This is consistent with the previous

analysis of the molecular structure in Marvin software, where the interactions will be distinct since in the case of LP_rFFD-PEG the OH groups are predominantly anionic whereas in the case of A β Peplnib the opposite is verified. It was also previously described in Michel et al. (2006) that the measurement of the mean count rate is often affected by structural alterations which may justify the decreasing phase in the case of A β Peplnib. With the study of DMPC/cholesterol phase diagram, the fact that the co-existence of the two phases, L_d (chol molecules distance the hydrocarbon core) + L_o (chol packed phospholipid molecules), between molar percentages of chol from 10 to 30% can influence the way lipids are organized and compacted or expanded by the predominance of one of the phases (Almeida, Vaz, and Thompson 1992). In the literature it is not yet well defined whether the phase transition temperature should increase or decrease in chol presence, but both cases have been described (Surovtsev and Dzuba 2014; Serro et al. 2014).

Drug Location Studies by Fluorescence Quenching

The peptides membrane location was assessed by steady-state fluorescence quenching using the DPH probe (Pinheiro et al. 2013). The efficiency of peptides to quench the fluorophore can be related to its proximity to the probe, providing the location and orientation of the peptides into the membrane. Figure 14 shows the Stern-Volmer plots of the DPH probe in LUVs of DMPC (for both peptides) and DMPC:Chol (only for A β Peplnib), with increasing concentrations of both peptides (quencher) obtained by steady state fluorescent measurements.

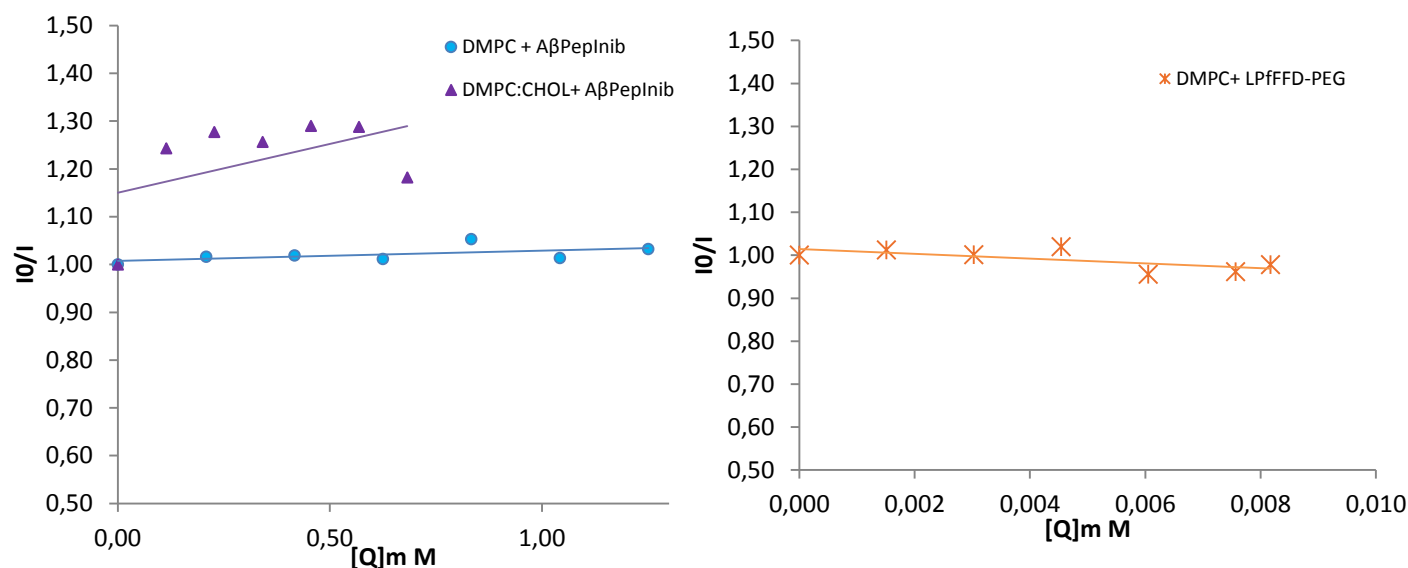


Figure 14 - Stern-Volmer plots obtained by steady-state fluorescence measurements of DPH in LUVs of DMPC (for both peptides), and DMPC:Chol (only for AβPeplnib) under physiological conditions (pH 7.4; 37 °C).

In the table below are present the Stern-Volmer constant (K_{sv}), for both systems, which were obtained through the corresponding slopes of DPH probe, at pH 7.4 and 37 °C.

Table 8 - Values of Stern-Volmer constant at $T = 37$ °C obtained for peptides in DMPC labeled with DPH probe. (n=2)

	K_{sv} (M^{-1}) AβPeplnib	K_{sv} (M^{-1}) LPfFFD-PEG
	DPH	DPH
DMPC	0.023	-3.27
DMPC:CHOL	0.51	-

From the analysis of table 8 it is possible to conclude that the K_{sv} values of all systems are very close to zero, which may indicate that both peptides, at physiological conditions, have a preferential location in a surface region of the bilayer, and near the polar region, without affinity for the probe studied. The close proximity between the probe and the peptide leads to a decrease in the fluorescence intensity and consequent increase in the K_{sv} value (Pineiro et al. 2013) may justify these observations. According to the determined pK_a values, the membrane location of peptides can be correlated with its structure, lipophilicity and ionization degree. According to the Marvin Software the AβPeplnib is mainly positively charged at pH 7.4, which makes it possible to establish electrostatic interactions with the phosphate group

present in choline. On the other hand, the peptide LP_rFFD-PEG is present mainly as zwitterionic species, with predominance of negatively charged groups. These in turn facilitates the binding to the headgroup of the phospholipids, since the anions will establish interaction with the ammonium group and the cations with the phosphate group of DMPC. By adding cholesterol molecules to the A β PepInib, the observed increase in the value of K_{sv} may be explained by the higher organization level and the degree of lipid packing of the membrane. Probably a similar result would be obtained in relation to the other peptide, since the same decrease is perceived in other studies (Neves et al. 2016).

Chapter 5

CONCLUDING REMARKS AND FUTURE PERSPECTIVES

LP_rFFD-PEG and A β PepInib are potential drug candidates for AD. Promising results related to inhibition of formation of A β aggregates were obtained. Ultimately these drug candidates may prevent and delay the progression of AD. Since their site of action is located in the brain, they need to cross the BBB. Thus the interactions of these peptides with biomembrane models are of paramount importance. In the present work it was concluded that both peptides interact with the membrane models changing their properties.

By the results analysis it was possible to observe that the peptides have a similar behavior between them interacting with the membrane models mainly by electrostatic interactions. It should be noted that the addition of chol to the model introduces a greater complexity due to the *condensation effect* on the membrane, which led to a decrease in K_p values and a significant variation of the phase transition temperature. With the fluorescence quenching analysis it was possible to understand how deep the peptides penetrate the membrane, and it was found that both had no affinity for the probe used, which may indicate a preferential location in the surface region of the bilayer.

In the future the study of addition of sphingomyelin to mimetic biomembrane models to better simulate *in vivo* conditions should be carried out. Also, different pH conditions and analysis of fluorescence quenching with another probes with different locations, such as TMA-DPH, would improve the design of new molecules more efficient in AD treatment.

REFERENCES

- A. Armstrong, Richard. 2014. 'Review paper: 'A critical analysis of the 'amyloid cascade hypothesis'', *Folia Neuropathologica*, 52: 211-25.
- Aileen Funke, Susanne, and Dieter Willbold. 2012. 'Peptides for therapy and diagnosis of Alzheimer's disease', *Current pharmaceutical design*, 18: 755-67.
- Alessandrini, Andrea, and Paolo Facci. 2014. 'Phase transitions in supported lipid bilayers studied by AFM', *Soft matter*, 10: 7145-64.
- Almeida, Paulo FF, Winchil LC Vaz, and TE Thompson. 1992. 'Lateral diffusion in the liquid phases of dimyristoylphosphatidylcholine/cholesterol lipid bilayers: a free volume analysis', *Biochemistry*, 31: 6739-47.
- Alzheimer's, Association. 2014. '2014 Alzheimer's disease facts and figures', *Alzheimer's & Dementia*, 10: e47-e92.
- Baciu, Magdalena, Sarra C Sebai, Oscar Ces, Xavier Mulet, James A Clarke, Gemma C Shearman, Robert V Law, Richard H Templer, Christophe Plisson, and Christine A Parker. 2006. 'Degradative transport of cationic amphiphilic drugs across phospholipid bilayers', *Philosophical Transactions of the Royal Society of London A: Mathematical, Physical and Engineering Sciences*, 364: 2597-614.
- Baginski, Maciej, Jacek Czub, and Kamil Sternal. 2006. 'Interaction of amphotericin B and its selected derivatives with membranes: molecular modeling studies', *The Chemical Record*, 6: 320-32.
- Binkley, J, and M Libarondi. 2010. 'Comparing the capabilities of time-of-flight and quadrupole mass spectrometers', *Current Trends in Mass Spectrometry*: 1-5.
- Blume, Alfred, and Andreas Kerth. 2013. 'Peptide and protein binding to lipid monolayers studied by FT-IRRA spectroscopy', *Biochimica et Biophysica Acta (BBA) - Biomembranes*, 1828: 2294-305.
- Böhm, Hans-Joachim, David Banner, Stefanie Bendels, Manfred Kansy, Bernd Kuhn, Klaus Müller, Ulrike Obst-Sander, and Martin Stahl. 2004. 'Fluorine in medicinal chemistry', *ChemBioChem*, 5: 637-43.
- Butterfield, D. Allan, and Christopher M. Lauderback. 2002. 'Lipid peroxidation and protein oxidation in Alzheimer's disease brain: potential causes and consequences involving amyloid β -peptide-associated free radical oxidative stress^{1,2}', *Free Radical Biology and Medicine*, 32: 1050-60.
- Caracciolo, Giulio, and Heinz Amenitsch. 2012. 'Cationic liposome/DNA complexes: from structure to interactions with cellular membranes', *European Biophysics Journal*, 41: 815-29.
- Chacon, MA, MI Barria, C Soto, and NC Inestrosa. 2004. '[β]-sheet breaker peptide prevents A [β]-induced spatial memory impairments with partial reduction of amyloid deposits', *Molecular psychiatry*, 9: 953.
- Chan, Eric C. Y., Swee-Lee Yap, Aik-Jiang Lau, Pay-Chin Leow, Ding-Fung Toh, and Hwee-Ling Koh. 2007. 'Ultra-performance liquid chromatography/time-of-flight mass spectrometry based metabolomics of raw and steamed Panax notoginseng', *Rapid Communications in Mass Spectrometry*, 21: 519-28.
- Chen, Kai Loon, and Geoffrey D Bothun. 2013. "Nanoparticles meet cell membranes: probing nonspecific interactions using model membranes." In.: ACS Publications.
- Dawkins, E., and D. H. Small. 2014. 'Insights into the physiological function of the β -amyloid precursor protein: beyond Alzheimer's disease', *J Neurochem*, 129: 756-69.
- De Bona, Paolo, Maria Laura Giuffrida, Filippo Caraci, Agata Copani, Bruno Pignataro, Francesco Attanasio, Sebastiano Cataldo, Giuseppe Pappalardo, and Enrico Rizzarelli.

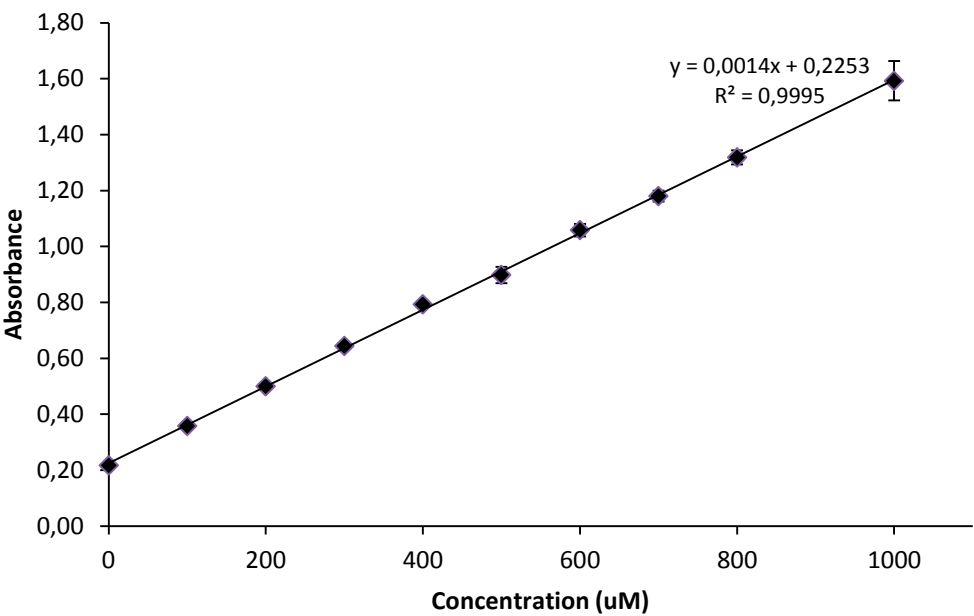
2009. 'Design and synthesis of new trehalose-conjugated pentapeptides as inhibitors of A β (1–42) fibrillogenesis and toxicity', *Journal of Peptide Science*, 15: 220-28.
- Deleu, Magali, Jean-Marc Crowet, Mehmet N. Nasir, and Laurence Lins. 2014. 'Complementary biophysical tools to investigate lipid specificity in the interaction between bioactive molecules and the plasma membrane: A review', *Biochimica et Biophysica Acta (BBA) - Biomembranes*, 1838: 3171-90.
- Dua, JS, AC Rana, and AK Bhandari. 2012. 'Liposome: methods of preparation and applications', *Int J Pharm Stud Res*, 3: 14-20.
- Eeman, Marc, and Magali Deleu. 2010. 'From biological membranes to biomimetic model membranes', *Biotechnologie, Agronomie, Société et Environnement*, 14: 719.
- Eftink, Maurice R. 2002. 'Fluorescence quenching: theory and applications.' in, *Topics in fluorescence spectroscopy* (Springer).
- Engberg, Oskar, Henrik Nurmi, Thomas KM Nyholm, and J Peter Slotte. 2015. 'Effects of Cholesterol and Saturated Sphingolipids on Acyl Chain Order in 1-Palmitoyl-2-oleoyl-sn-glycero-3-phosphocholine Bilayers: A Comparative Study with Phase-Selective Fluorophores', *Langmuir*, 31: 4255-63.
- Esparza, Caitlin. 'Cerebrovascular and Blood-Brain Barrier Impairments in Huntington's Disease: Potential Implications for Its Pathophysiology'.
- Freire, Joao M, Marco M Domingues, Joana Matos, Manuel N Melo, Ana Salomé Veiga, Nuno C Santos, and Miguel ARB Castanho. 2011. 'Using zeta-potential measurements to quantify peptide partition to lipid membranes', *European Biophysics Journal*, 40: 481-87.
- Frydman-Marom, Anat, Ronit Shaltiel-Karyo, Sari Moshe, and Ehud Gazit. 2011. 'The generic amyloid formation inhibition effect of a designed small aromatic β -breaking peptide', *Amyloid*, 18: 119-27.
- Gabathuler, Reinhard. 2010. 'Approaches to transport therapeutic drugs across the blood–brain barrier to treat brain diseases', *Neurobiology of disease*, 37: 48-57.
- Handattu, Shaila P, David W Garber, Candyce E Monroe, Thomas van Groen, Inga Kadish, Gaurav Nayyar, Dongfeng Cao, Mayakonda N Palgunachari, Ling Li, and GM Anantharamaiah. 2009. 'Oral apolipoprotein AI mimetic peptide improves cognitive function and reduces amyloid burden in a mouse model of Alzheimer's disease', *Neurobiology of disease*, 34: 525-34.
- Hansen, R. A., G. Gartlehner, A. P. Webb, L. C. Morgan, C. G. Moore, and D. E. Jonas. 2008. 'Efficacy and Safety of Donepezil, Galantamine, and Rivastigmine for the Treatment of Alzheimer's Disease: A Systematic Review and Meta-Analysis', *Clin Interv Aging*, 3: 211-25.
- Hardy, John, and Dennis J. Selkoe. 2002. 'The Amyloid Hypothesis of Alzheimer's Disease: Progress and Problems on the Road to Therapeutics', *Science*, 297: 353-56.
- Heimburg, Thomas. 2007. 'Membrane Structure.' in, *Thermal Biophysics of Membranes* (Wiley-VCH Verlag GmbH & Co. KGaA).
- Jack, C. R., D. S. Knopman, W. J. Jagust, R. C. Petersen, M. W. Weiner, P. S. Aisen, L. M. Shaw, P. Vemuri, H. J. Wiste, S. D. Weigand, T. G. Lesnick, V. S. Pankratz, M. C. Donohue, and J. Q. Trojanowski. 2013. 'Update on hypothetical model of Alzheimer's disease biomarkers', *Lancet Neurol*, 12: 207-16.
- Jeffrey, Phil, and Scott Summerfield. 2010. 'Assessment of the blood–brain barrier in CNS drug discovery', *Neurobiology of disease*, 37: 33-37.
- Jiang, Jingkun, Günter Oberdörster, and Pratim Biswas. 2009. 'Characterization of size, surface charge, and agglomeration state of nanoparticle dispersions for toxicological studies', *Journal of Nanoparticle Research*, 11: 77-89.
- Joye, Iris J, Gabriel Davidov-Pardo, Richard D Ludescher, and David J McClements. 2015. 'Fluorescence quenching study of resveratrol binding to zein and gliadin: towards a

- more rational approach to resveratrol encapsulation using water-insoluble proteins', *Food Chemistry*, 185: 261-67.
- Kim, Jin-Seok. 2016. 'Liposomal drug delivery system', *Journal of Pharmaceutical Investigation*, 46: 387-92.
- Knobloch, Jacqueline, Daniel K. Suhendro, Julius L. Zieleniecki, Joseph G. Shapter, and Ingo Köper. 2015. 'Membrane–drug interactions studied using model membrane systems', *Saudi Journal of Biological Sciences*, 22: 714-18.
- Koynova, Rumiana, and Martin Caffrey. 1998. 'Phases and phase transitions of the phosphatidylcholines', *Biochimica et Biophysica Acta (BBA) - Reviews on Biomembranes*, 1376: 91-145.
- Krause, Martin R, Trevor A Daly, Paulo F Almeida, and Steven L Regen. 2014. 'Push–pull mechanism for lipid raft formation', *Langmuir*, 30: 3285-89.
- Kwon, Younggil. 2001. *Handbook of essential pharmacokinetics, pharmacodynamics and drug metabolism for industrial scientists* (Springer Science & Business Media).
- Lantos, Peter L., Philip J. Luthert, Diane Hanger, Brain H. Anderton, Michael Mullan, and Martin Rossor. 1992. 'Familial Alzheimer's disease with the amyloid precursor protein position 717 mutation and sporadic Alzheimer's disease have the same cytoskeletal pathology', *Neuroscience Letters*, 137: 221-24.
- Lasic, Danilo D. 1997. *Liposomes in gene delivery* (CRC press).
- Leinenga, Gerhard, Christian Langton, Rebecca Nisbet, and Jurgen Gotz. 2016. 'Ultrasound treatment of neurological diseases [mdash] current and emerging applications', *Nat Rev Neurol*, 12: 161-74.
- Lesné, S. E., M. A. Sherman, M. Grant, M. Kuskowski, J. A. Schneider, D. A. Bennett, and K. H. Ashe. 2013. 'Brain amyloid- β oligomers in ageing and Alzheimer's disease', *Brain*, 136: 1383-98.
- Li, Jia, John M Butler, Yuping Tan, Hua Lin, Stephanie Royer, Lynne Ohler, Thomas A Shaler, Joanna M Hunter, Daniel J Pollart, and Joseph A Monforte. 1999. 'Single nucleotide polymorphism determination using primer extension and time-of-flight mass spectrometry', *Electrophoresis*, 20: 1258-65.
- Lim, JitKang, Swee Pin Yeap, Hui Xin Che, and Siew Chun Low. 2013. 'Characterization of magnetic nanoparticle by dynamic light scattering', *Nanoscale research letters*, 8: 381.
- Lockman. 2002. 'Nanoparticle Technology for Drug Delivery Across the Blood-Brain Barrier', *Drug Development and Industrial Pharmacy*, 28: 1-13.
- Loureiro, Joana A, Rosa Crespo, Hans Börner, Pedro M Martins, Fernando A Rocha, Manuel Coelho, M Carmo Pereira, and Sandra Rocha. 2014. 'Fluorinated beta-sheet breaker peptides', *Journal of Materials Chemistry B*, 2: 2259-64.
- Lúcio, Marlene, Cláudia Nunes, Diana Gaspar, Helena Ferreira, José L. F. C. Lima, and Salette Reis. 2009. 'Antioxidant Activity of Vitamin E and Trolox: Understanding of the Factors that Govern Lipid Peroxidation Studies In Vitro', *Food Biophysics*, 4: 312-20.
- M. Prince, A. Wimo, M. Guerchet, G.C. Ali, Y.-T. Wu, M. Prina. 2015. 'World Alzheimer Report 2015. The Global Impact of Dementia. An analysis of prevalence, incidence, costs and trends', *Alzheimer's Disease International, London (2015) World Alzheimer's Report*
- Magalhães, Luís M, Cláudia Nunes, Marlene Lúcio, Marcela A Segundo, Salette Reis, and José LFC Lima. 2010. 'High-throughput microplate assay for the determination of drug partition coefficients', *nature protocols*, 5: 1823.
- Magarkar, Aniket, Vivek Dhawan, Paraskevi Kallinteri, Tapani Viitala, Mohammed Elmowafy, Tomasz Róg, and Alex Bunker. 2014. 'Cholesterol level affects surface charge of lipid membranes in saline solution', *Scientific reports*, 4: 5005.
- Michel, Nicolas, Anne-Sylvie Fabiano, Ange Polidori, Robert Jack, and Bernard Pucci. 2006. 'Determination of phase transition temperatures of lipids by light scattering', *Chemistry and physics of lipids*, 139: 11-19.

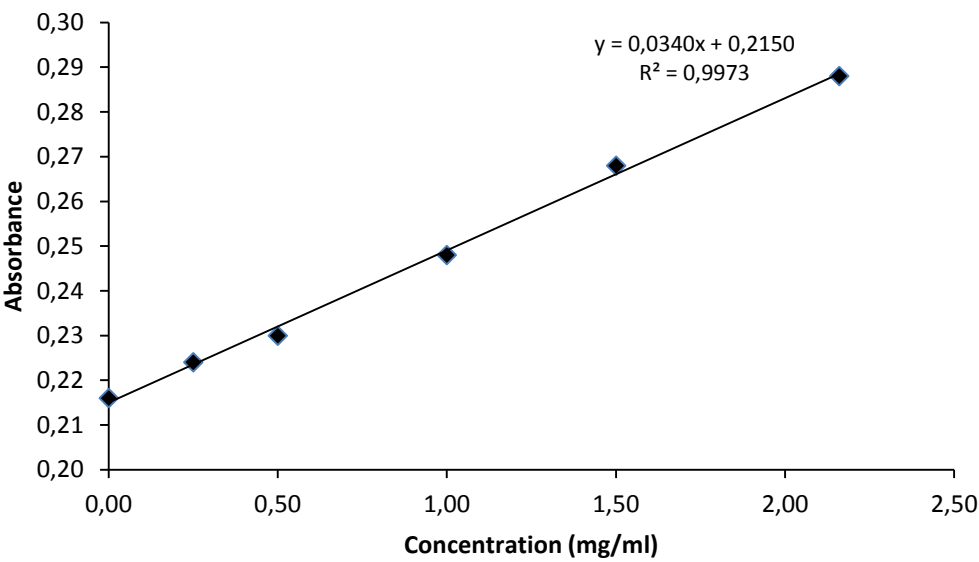
- Mufamadi, Maluta S, Yahya E Choonara, Pradeep Kumar, Lisa C du Toit, Girish Modi, Dinesh Naidoo, Sunny E Iyuke, and Viness Pillay. 2016. 'Functionalized Nanolipobubbles Embedded Within a Nanocomposite Hydrogel: a Molecular Bio-imaging and Biomechanical Analysis of the System', *AAPS PharmSciTech*: 1-15.
- Nag, Sukriti. 2003. 'Morphology and Molecular Properties of Cellular Components of Normal Cerebral Vessels.' in Sukriti Nag (ed.), *The Blood-Brain Barrier: Biology and Research Protocols* (Humana Press: Totowa, NJ).
- Neves, AR, C Nunes, H Amenitsch, and S Reis. 2016. 'Effects of resveratrol on the structure and fluidity of lipid bilayers: a membrane biophysical study', *Soft matter*, 12: 2118-26.
- Nordberg, Agneta. 2004. 'PET imaging of amyloid in Alzheimer's disease', *The Lancet Neurology*, 3: 519-27.
- Nussbaum, Justin M, Matthew E Seward, and George S Bloom. 2013. 'Alzheimer disease: a tale of two prions', *Prion*, 7: 14-19.
- Papadopoulou, Athina, Rebecca J Green, and Richard A Frazier. 2005. 'Interaction of flavonoids with bovine serum albumin: a fluorescence quenching study', *Journal of Agricultural and Food Chemistry*, 53: 158-63.
- Peetla, Chiranjeevi, Andrew Stine, and Vinod Labhasetwar. 2009. 'Biophysical Interactions with Model Lipid Membranes: Applications in Drug Discovery and Drug Delivery', *Molecular Pharmaceutics*, 6: 1264-76.
- Pinheiro, Marina, Mariana Arêde, João M Caio, Cristina Moiteiro, Marlene Lúcio, and Salette Reis. 2013. 'Drug-membrane interaction studies applied to N'-acetyl-rifabutin', *European Journal of Pharmaceutics and Biopharmaceutics*, 85: 597-603.
- Popovska, Olga. 2014. 'An overview: methods for preparation and characterization of liposomes as drug delivery systems', *International Journal of Pharmaceutical and Phytopharmacological Research*, 3.
- Purser, Sophie, Peter R Moore, Steve Swallow, and Véronique Gouverneur. 2008. 'Fluorine in medicinal chemistry', *Chemical Society Reviews*, 37: 320-30.
- Rocha, Sandra, Andreas F Thünemann, Maria do Carmo Pereira, Manuel Coelho, Helmuth Möhwald, and Gerald Brezesinski. 2008. 'Influence of fluorinated and hydrogenated nanoparticles on the structure and fibrillogenesis of amyloid beta-peptide', *Biophysical chemistry*, 137: 35-42.
- Rodrigues, Catarina, Paula Gameiro, Salette Reis, JLFC Lima, and Baltazar de Castro. 2001. 'Spectrophotometric determination of drug partition coefficients in dimyristoyl-l- α -phosphatidylcholine/water: a comparative study using phase separation and liposome suspensions', *Analytica chimica acta*, 428: 103-09.
- Rothfield, Lawrence. 1971. '1 - BIOLOGICAL MEMBRANES: AN OVERVIEW AT THE MOLECULAR LEVEL.' in, *Structure and Function of Biological Membranes* (Academic Press).
- Sadowski, Marcin, Joanna Pankiewicz, Henrieta Scholtzova, James A Ripellino, Yongsheng Li, Stephen D Schmidt, Paul M Mathews, John D Fryer, David M Holtzman, and Einar M Sigurdsson. 2004. 'A synthetic peptide blocking the apolipoprotein E/ β -amyloid binding mitigates β -amyloid toxicity and fibril formation in vitro and reduces β -amyloid plaques in transgenic mice', *The American journal of pathology*, 165: 937-48.
- Santoso, Steve, Wonmuk Hwang, Hyman Hartman, and Shuguang Zhang. 2002. 'Self-assembly of surfactant-like peptides with variable glycine tails to form nanotubes and nanovesicles', *Nano Letters*, 2: 687-91.
- Saraiva, Cláudia, Catarina Praça, Raquel Ferreira, Tiago Santos, Lino Ferreira, and Liliana Bernardino. 2016. 'Nanoparticle-mediated brain drug delivery: Overcoming blood-brain barrier to treat neurodegenerative diseases', *Journal of Controlled Release*, 235: 34-47.
- Scandroglio, F., J. K. Venkata, N. Loberto, S. Prioni, E. H. Schuchman, V. Chigorno, A. Prinetti, and S. Sonnino. 2008. 'LIPID CONTENT OF BRAIN, OF BRAIN MEMBRANE LIPID

- DOMAINS, AND OF NEURONS FROM ACID SPHINGOMYELINASE DEFICIENT MICE (ASMKO)', *J Neurochem*, 107: 329-38.
- Seddon, Annela M., Duncan Casey, Robert V. Law, Antony Gee, Richard H. Templer, and Oscar Ces. 2009. 'Drug interactions with lipid membranes', *Chemical Society Reviews*, 38: 2509-19.
- Serro, AP, R Galante, A Kozica, P Paradiso, AMPS Goncalves Da Silva, KV Luzyanin, AC Fernandes, and B Saramago. 2014. 'Effect of tetracaine on DMPC and DMPC+ cholesterol biomembrane models: Liposomes and monolayers', *Colloids and Surfaces B: Biointerfaces*, 116: 63-71.
- Soto, Claudio, Mark S Kindy, Marc Baumann, and Blas Frangione. 1996. 'Inhibition of Alzheimer's amyloidosis by peptides that prevent β -sheet conformation', *Biochemical and biophysical research communications*, 226: 672-80.
- Spuch, C., and C. Navarro. 2011. 'Liposomes for Targeted Delivery of Active Agents against Neurodegenerative Diseases (Alzheimer's Disease and Parkinson's Disease)', *J Drug Deliv*, 2011.
- Stahl, S.M., and N. Muntner. 2013. *Stahl's Essential Psychopharmacology: Neuroscientific Basis and Practical Applications* (Cambridge University Press).
- Sun, Na, Susanne Aileen Funke, and Dieter Willbold. 2012. 'Mirror image phage display—Generating stable therapeutically and diagnostically active peptides with biotechnological means', *Journal of biotechnology*, 161: 121-25.
- Surovtsev, NV, and SA Dzuba. 2014. 'Flexibility of phospholipids with saturated and unsaturated chains studied by Raman scattering: The effect of cholesterol on dynamical and phase transitions', *The Journal of chemical physics*, 140: 06B615_1.
- Szegedi, Viktor, Livia Fülöp, Tamás Farkas, E Rozsa, H Robotka, Zsolt Kis, Z Penke, Szatmár Horváth, Z Molnar, and Zsolt Datki. 2005. 'Pentapeptides derived from A β 1–42 protect neurons from the modulatory effect of A β fibrils—an in vitro and in vivo electrophysiological study', *Neurobiology of disease*, 18: 499-508.
- Taly, Antoine, Laura Baciou, and Pierre Sebban. 2002. 'The DMPC lipid phase transition influences differently the first and the second electron transfer reactions in bacterial reaction centers', *FEBS letters*, 532: 91-96.
- Török, Marianna, Mohammed Abid, Shilpa C Mhadgut, and Béla Török. 2006. 'Organofluorine inhibitors of amyloid fibrillogenesis', *Biochemistry*, 45: 5377-83.
- van Meer, G., D. R. Voelker, and G. W. Feigenson. 2008. 'Membrane lipids: where they are and how they behave', *Nat Rev Mol Cell Biol*, 9: 112-24.
- Vieira, Débora B, and Lionel F Gamarra. 2016. 'Getting into the brain: liposome-based strategies for effective drug delivery across the blood–brain barrier', *International Journal of Nanomedicine*, 11: 5381.
- Villemagne, Victor L., Samantha Burnham, Pierrick Bourgeat, Belinda Brown, Kathryn A. Ellis, Olivier Salvado, Cassandra Szeke, S. Lance Macaulay, Ralph Martins, Paul Maruff, David Ames, Christopher C. Rowe, and Colin L. Masters. 2013. 'Amyloid β deposition, neurodegeneration, and cognitive decline in sporadic Alzheimer's disease: a prospective cohort study', *The Lancet Neurology*, 12: 357-67.
- Wang, Z. L. 2000. 'Transmission Electron Microscopy of Shape-Controlled Nanocrystals and Their Assemblies', *The Journal of Physical Chemistry B*, 104: 1153-75.
- Wu, Chun, Matthew Biancalana, Shohei Koide, and Joan-Emma Shea. 2009. 'Binding modes of thioflavin-T to the single-layer β -sheet of the peptide self-assembly mimics', *Journal of molecular biology*, 394: 627-33.
- Zhao, Yuhai, Surjyadipta Bhattacharjee, Brandon M. Jones, James M. Hill, Christian Clement, Kumar Sambamurti, Prerna Dua, and Walter J. Lukiw. 2015. 'Beta-Amyloid Precursor Protein (β APP) Processing in Alzheimer's Disease (AD) and Age-Related Macular Degeneration (AMD)', *Molecular Neurobiology*, 52: 533-44.

Appendix



Appendix 1 - Calibration Curve of ABPeptInib using BioTek® Synergy 2 Multi-Mode Reader (n=3)



Appendix 2 - Calibration Curve of LPfFFD-PEG using BioTek® Synergy 2 Multi-Mode Reader (n=2)